

# CHAPTER ONE

## Basic concepts of coating

### 1.1 Introduction:

A coating is a covering that is applied to the surface of an object, usually referred to as the substrate. The purpose of applying the coating may be decorative, functional, or both. The coating itself may be an all-over coating, completely covering the substrate, or it may only cover parts of the substrate. An example of all of these types of coating is a product label on many drinks bottles- one side has an all-over functional coating (the adhesive) and the other side has one or more decorative coatings in an appropriate pattern (the printing) to form the words and images. Paints and lacquers are coatings that mostly have dual uses of protecting the substrate and being decorative, although some artist's paints are only for decoration, and the paint on large industrial pipes is presumably only for the function of preventing corrosion, (Felton, Linda A, Porter, Stuart C. 2013).

Functional coatings may be applied to change the surface properties of the substrate, such as adhesion, wettability, corrosion resistance, or wear resistance. In other cases, e.g. semiconductor device fabrication (where the substrate is a wafer), the coating adds a completely new property such as a magnetic response or electrical conductivity and forms an essential part of the finished product.

A major consideration for most coating processes is that the coating is to be applied at a controlled thickness, and a number of different processes are in use to achieve this control, ranging from a simple brush for painting a wall, to some very expensive machinery applying coatings in the electronics industry. A further consideration for 'non-all-over' coatings is that control is needed as to where the

coating is to be applied. A number of these non-all-over coating processes are printing processes.

Many industrial coating processes involve the application of a thin film of functional material to a substrate, such as paper, fabric, film, foil, or sheet stock. If the substrate starts and ends the process wound up in a roll, the process may be termed "roll-to-roll" or "web-based" coating. A roll of substrate, when wound through the coating machine, is typically called a web. Coatings may be applied as liquids, gases or solids (Felton, Linda A; Porter, Stuart C .2013).

The expressions "Thin films" and "Semiconductor technology" are almost synonyms. It is true, there is some semiconductor technology that does not need thin films but not much comes to mind right away.

There is, however, quite a bit of thin film technology outside of semiconductor technology, e.g., in optics. In fact, thin film technology is far older than semiconductor technology. In ancient times, for example, people already knew how to beat gold into a thin film ( $< 1 \mu\text{m}$  thickness) with hammers and knew how to use this "gold leaf" for coating all kinds of stuff.

Thin film technology involves deposition of individual molecules or atoms.

Thick film technology involves deposition of particles.

Painting thus is thick film technology, and evaporation is thin film technology. Good enough, but what about beating gold with hammers to sheets with a thickness of 5 nm, or depositing 100  $\mu\text{m}$  of Ag or Cr on a metal galvanically, atom by atom, to be sure.

All in all, there is no natural distinction between "thick" and "thin", it always has to be practical. In what we look at here, we consider in a first approximation thin films to be typically thinner than 1  $\mu\text{m}$ , or if needs be a few  $\mu\text{m}$ . Let's get an idea of what that means: one of the smallest things we still can see and touch is a human hair. They come fine and coarse, but a typical thickness value is (30 - 50)  $\mu\text{m}$ .

Having defined what is meant by terminus (thin Film), we may now turn to the calculation of the transmittance and reflectance of a thin film embedded between two media. The thickness less than a few micrometers .In this case, the mechanical stability of the system cannot be guaranteed, so that the film is deposited on to another solid material, which forms the substrate, Figure (1-1),below shows transmission,reflectance of the thin film.(O.Stenzel, 2005).

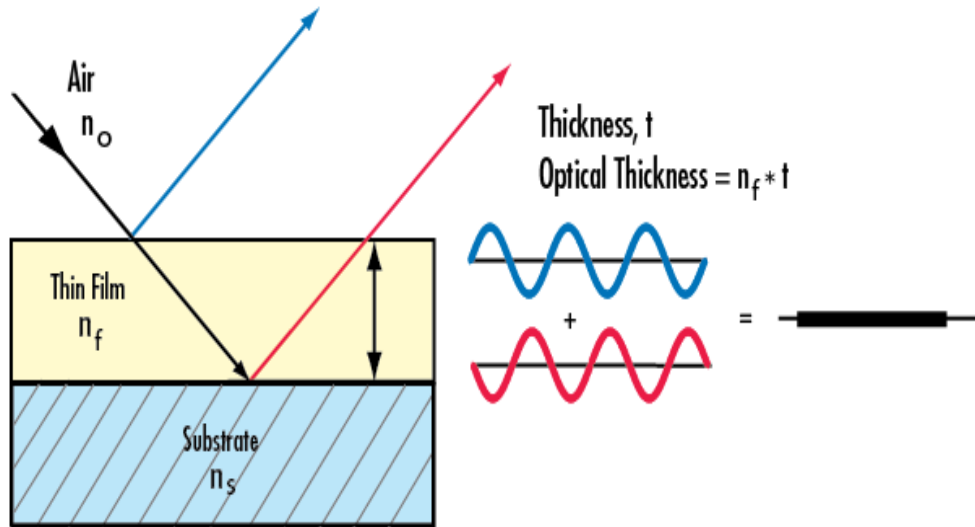


**Figure (1.1): Transmission,reflectance of thin film.**

Thin film materials have become technologically important in recent years. Some examples are:

- Microelectronic Integrated Circuits
- Magnetic Information Storage Systems
- Optical Coatings
- Wear Resistant Coatings
- Corrosion Resistant Coatings

Motivation for the use of materials in thin film form:

- Need for small-scale devices (I.C.'s, magnetic storage)
- Physical properties that are scale-dependent (optical filters)
- Cost benefits (use small amounts of expensive materials forcoatings)

Although one typically think of thin film based devices in terms of their electronic, magnetic or optical properties, many such devices are limited by their mechanical properties important to understand mechanical properties of thin films.(Li, J. and Zhang, J.Z., 2009).

The transmittance and reflectance of a thin film embedded between two media, the thickness less than a few micrometers. In this case, the mechanical stability of the system cannot be guaranteed, so that the film is deposited on to another solid material, which forms the substrate. Figure (1-1) shows the transmittance, reflectance of the thin film.(O.Stenzel, 2005).

## **1.2 The study objectives:**

The main objectives of this study are to produce multilayer thin films from Phinixazon, Rohdamine, and Coumarin, and the determination of some optical properties for these thin films; such as reflectivity, transmittance, refractive index and absorption coefficient in order to determine the validity of these thin films to be used as optical components for certain wavelengths .

## **1.3 Thesis structure:**

The first chapter of this thesis covered the basic concepts of thin films and coating (history, types, properties).

The second chapter covered the multilayers thin films coating and technology of deposition of thin films, and also the general theory of filters.

In chapter three the detailed description of the experimental work is presented.

Chapter four deals with results, discussion, conclusions, and future work.

## **1.4 History of thin films:**

The oldest evidence of painting was left by primitive peoples. Cave dwellers and hunters left paintings of the animals that they hunted. Paintings in caves have

survived because of their protected locations. Most cave paintings used the colors black, red, and yellow. Chemical analysis of these early paintings has shown that the main pigments used were iron and manganese oxides. To form applicable paints, the pigments were possibly mixed with egg white, animal fats, plant sap, or water. (Thomas,N.L., 1991).

The resulting mixture of binder-containing pigments could then be applied to cave walls. During the period 3000–600 BC, many paint-making advances were made by the Egyptians. They not only developed pigments with a wider range of colors but are also credited with producing the first synthetic pigment (Egyptian Blue) and developing the first lake pigments. Preservative paints and varnishes were also used during this time. Drying oils as part of varnishes were used during the period 600 BC–400 AD by the Greeks and Romans. In the tenth century AD, Theophilus describes a varnish made by heating amber resin with linseed oil. Varnish was used to protect painting on wood during the middle Ages. Pigments were suspended in a varnish like the one described by Theophilus in order to make a more durable paints.

For hundreds of years, paint formulations were handed down from one generation to the next and were often carefully guarded. Paints were produced in small batches, with the procedure being a relatively expensive one and the product not affordable to many.

However, the demand for paint and coatings became great enough that by the late eighteenth and early nineteenth century it became profitable to make paint for wider consumption.

The first paint and varnish factories were established during the nineteenth century. The industrial revolution and the mass production of the automobile strongly influenced the growth of the paint and coatings industry. The need for anti-corrosive coatings as well as other special-purpose coatings, helped to accelerate the rate of scientific discovery. Titanium dioxide, the white pigment

that would replace white lead, was introduced in 1918. After the middle of the twentieth century, the natural oils that had been used in paint formulations were replaced by synthetic resins. Today's coatings manufacturers offer a wide variety of products to protect, decorate, and perform special functions on the surfaces of products ranging from children's toys to spacecraft.

In the later part of the twentieth century, society's growing environmental awareness has presented a new challenge to the paint and coatings industry—to produce coating products that meet the demands of manufacturers and consumers and at the same time comply with the government environmental constraints. Certain chemicals have been shown to be toxic and hazardous to humans and/or their environment. Regulatory agencies are setting strict standards with which coatings manufacturers need to comply. This has led to a greater interest in developing coatings such as those that use water instead of volatile organic compounds in their formulation and powdered coatings that are absolutely free solvent. ((Thomas, N.L., 1991).

At the End of 19th century - unusual properties of deposits on the walls of glass discharge tubes raised interest of researchers: optical & electrical properties. 1927: electron diffraction on thin films. 1930th - practical application: high reflectivity surface mirrors on non-conducting substrates.

1940th - vacuum and thin film (PVD) techniques, devices;

- electron microscopy.

1960th - in situ electron microscopy.

- Surface decoration.

- Ultrahigh vacuum technique;

- Surface analytical methods. Structure zone model: compilation of experimental results.

1970th - high resolution (also surface imaging) and analytical TEM.

- Chemical vapor deposition (CVD);

- Computer simulation: atom-by-atom structure building
- Molecular beam epitaxy (MBE);
- CERMET (nanocomposite) resistor films.

1980th - - atomic resolution surface imaging techniques: STM, AFM.

- Atomic layer epitaxy;
- Electron energy loss analysis - dedicated scanning TEM;

1990th - aberration corrected ultrahigh resolution analytical TEM.

2000th - advent of in situ techniques. (Peter B.Barna, 2005).

Although liquid crystal displays(LCDs) have been available for over half a century, they were always taken as niche market products because of their rather poor performance: small viewing angles, long response time, and lack of large-area panels. The situation has changed drastically since the availability of the active matrix (AM) LCDs, specially the amorphous silicon (a-Si: H) thin film transistor (TFT) driven LCDs. For example, worldwide revenue of the TFT LCD improved from about \$1 billion in 1989 to near \$110 billion in 2012. The main producers expanded from Japan to the surrounding Asia Pacific countries, such as South Korea, Taiwan, and China. The shipment of LCD TV units from 2011 to 2012 was predicted to increase by 9% to 225 million units. In the early mass production stage, thin film transistor liquid crystal displays (TFTLCDs) were used in high price products, such as computer monitors, games, and instruments. Later on, due to the gradual maturity of the production technology, TFT LCDs were applied to consumer electronics, such as TVs and mobile phones. At the same time, researchers were investigating new types of TFTs to solve some of the intrinsic device performance or production problems. Furthermore, applications of TFTs beyond pixel driving in the LCD have been explored. Therefore, this is a good time to review the history and progress of the TFT technology as well as to predict possible future development trends. (Yue Kuo. 2013).

## **Pre Mass Production of Large- Area TFT LCDs—Before 1990**

The TFT is a field effect transistor (FET). Its structure and operation principles are similar to those of the metal oxide field effect transistor (MOSFET), which is the most critical device component in modern integrated circuits (ICs). The development histories of TFTs and MOSFETs are similar, as shown in Fig. (1-1). The metal insulator semiconductor field effect transistor (MISFET) conceptually was born in 1925. The early popular TFT versions were made of compound semiconductors, such as CdS or CdSe. This kind of TFT has high field effect mobility,  $\mu_{\text{eff}}$ , e.g.,  $> 40 \text{ cm}^2/\text{Vs}$ . The CdSe TFT LCD was first demonstrated in 1973. However, mass production of this kind of LCD on large-area substrates has never been realized. Among many possible reasons, complications in controlling the compound semiconductor thin film material properties and device reliability over large areas are often discussed. The breakthrough in the field came from a report in 1979 of the first functional TFT made from hydrogenated amorphous silicon (a-Si: H) with a silicon nitride gate dielectric layer. Figure (1-3) shows (a) structure and (b) transfer characteristics of the first a-Si: H TFT. (Yue Kuo, 2013).



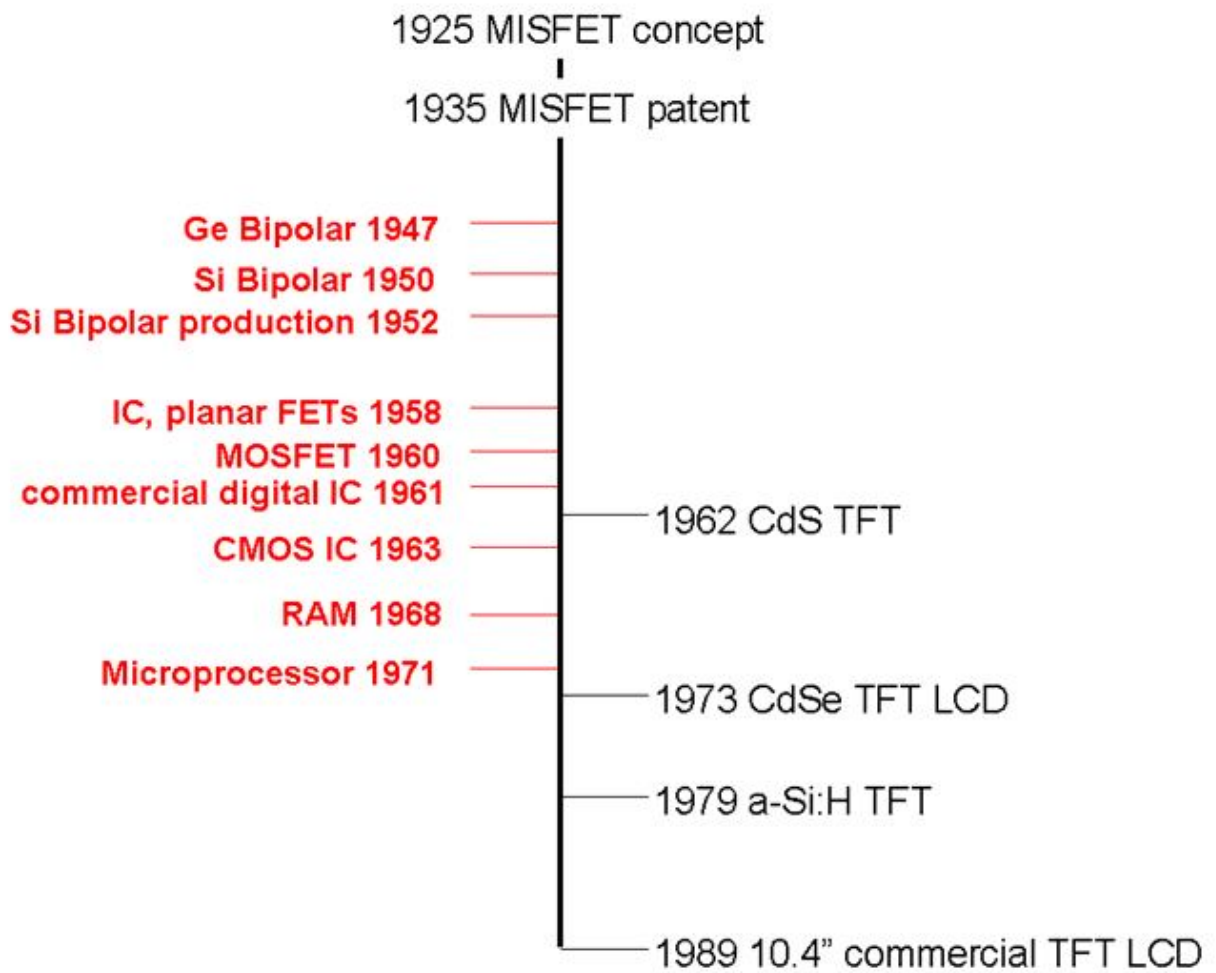
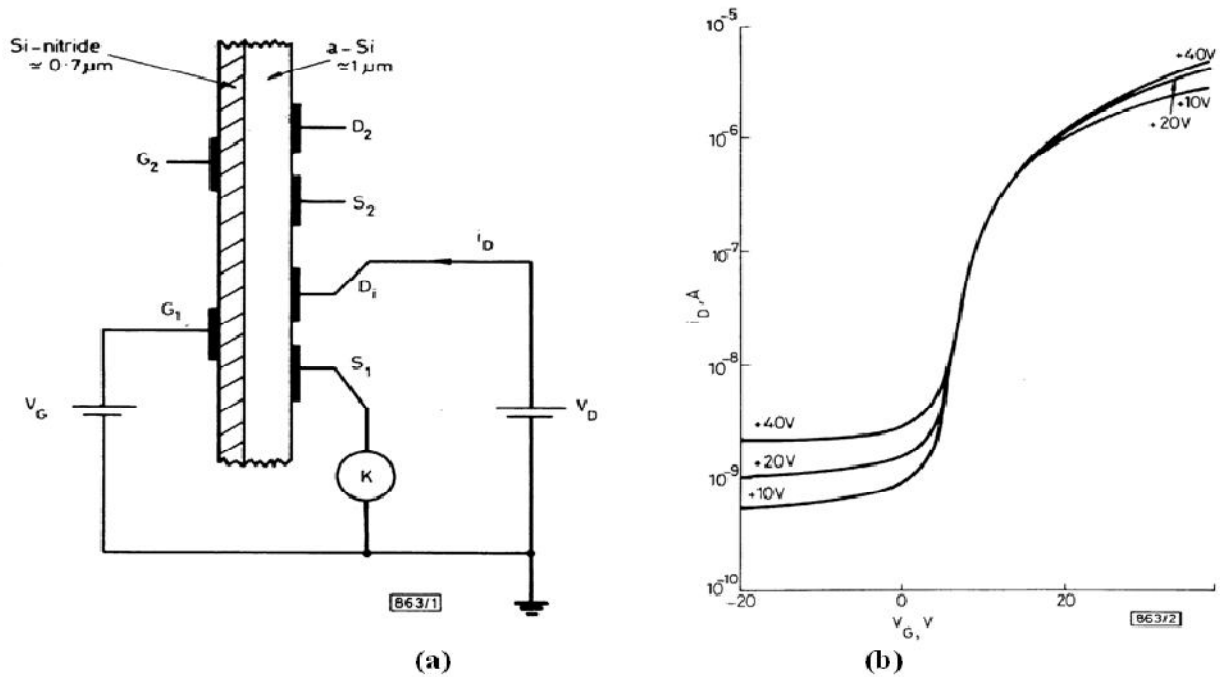


**Figure (1-2): History of TFT and IC development**



**Figures (1-3):(a) Si:H TFT structure and (b) transfer characteristics.**

### 1.5 Applications of thin films:

Although the study of thin film phenomena dates back well over a century, it is really only over the last four decades that they have been used to a significant extent in practical situations. The requirement of micro miniaturization made the use of thin and thick films virtually imperative. The development of computer technology led to a requirement for very high density storage techniques and it is this which has stimulated most of the research on the magnetic properties of thin films. Many thin film devices have been developed which have found themselves looking for an application. In general these devices have resulted from research into the physical properties of thin films.

Thin film materials have already been used in semiconductor devices, wireless communications, telecommunications, integrated circuits, rectifiers, transistors, solar cells, light-emitting diodes, photoconductors, light crystal displays, magneto-optic memories, audio and video systems, compact discs, electro-optic coatings, memories, multilayer capacitors, flat-panel displays, smart windows, computer

chips, magneto optic discs, lithography, micro- electromechanical systems and multifunctional emerging coatings, as well as other emerging cutting technologies.(Willey, Ronald R. 2007).

### **1.5.1 Data Storage:**

As the data storage density in cutting edge microelectronic devices continues to increase, the super paramagnetic effect poses a problem for magnetic data storage media. One strategy for overcoming this obstacle is the use of thermo mechanical data storage technology. In this approach, data is written by a nanoscale mechanical probe as an indentation on a surface, read by a transducer built into the probe, and then erased by the application of heat. An example of such a device is the IBM millipede, which uses a polymer thin film as the data storage medium. It is also possible; however, to use other kinds of media for thermo mechanical data storage and in the following work, we explore the possibility of using thin film Ni-Ti shape memory alloy (SMA). Previous work has shown that nanometer-scale indentations made in martensite phase Ni-Ti SMA thin films recover substantially upon heating. Issues such as repeated thermo mechanical cycling of indentations indent proximity and film thickness impact the practicability of this technique. While there are still problems to be solved, the experimental evidence and theoretical predictions show SMA thin films are an appropriate medium for thermo mechanical data storage. (Wendy C. Crone, Gordon A.Shaw2005).

### **1.5.2 Flat Panel Displays:**

The Flat Panel Display (FPD) fabrication environment is among the world's most competitive and technologically complex. Device designers and manufacturers continually strive to satisfy the worldwide consumer's appetite for larger displays, greater pixel resolution and feature-rich performance, all at a lower cost than the previous generation of technology. The need to control contamination in air, gas and liquid process streams is now a paramount focus of process engineers and designers. ((JEFFREY A. Hart. 2015).

### **1.5.3 Optoelectronic Devices:**

An optoelectronic thin-film chip, comprising at least one radiation-emitting region in an active zone of a thin-film layer and a lens disposed downstream of the radiation emitting region, said lens being formed by at least one partial region of the thin-film layer, the lateral extent of the lens being greater than the lateral extent of the radiation emitting region. The thin-film layer is provided for example by a layer sequence which is deposited epitaxial on a growth substrate and from which the growth substrate is at least partly removed. That is to say that the thickness of the substrate is reduced. In other words, the substrate is thinned. It is furthermore possible for the entire growth substrate to be removed from the thin-film layer. The thin-film layer has at least one active zone suitable for generating electromagnetic radiation. The active zone may be provided for example by a layer or layer sequence which has a p-n junction, a double heterostructure, a single quantum well structure or a multiple quantum well structure. Particularly preferably, the active zone has at least one radiation-emitting region. In this case, the radiation-emitting region is formed for example by a partial region of the active zone. Electromagnetic radiation is generated in said partial region of the active zone during operation of the optoelectronic thin-film chip.

(Aad, G., Abbott, B., Abdallah, et al, 2014).

### **1.5.4 Optical Coatings:**

An optical coating is one or more thin layers of material deposited on an optical component such as a lens or mirror, which alters the way in which the optic reflect and transmits light. One type of optical coating is an antireflection coating, which reduces unwanted reflections from surfaces and is commonly used on spectacle and photographic lenses. Another type is the high-reflector coating which can be used to produce mirrors which reflect greater than 99.99% of the light which falls on them. More complex optical coatings exhibit high reflection over some range

of wavelengths, and anti-reflection over another range, allowing the production of dichroic thin-film optical filters, in general filter can consist of multilayer coatings deposited onto one or both side of a substrate. (Suliman. E. M., 2007).

### **1.5.5 Thin film lithium ion batteries:**

They are similar to lithium ion batteries, but they are composed of thin materials, some only nanometers or micrometers thick, which allow for the finished battery to be just millimeters thick.

They have been developed and advanced primarily within the last decade. These batteries consist of a substrate, electrolyte, current collector, anode, cathode and a charge separator. There has been much research into the determination of the most effective components for this type of battery. It has been shown recently that even ordinary printer paper can be used as a charge separator and a substrate. These thin film batteries are an improvement on the common secondary or rechargeable lithium ion batteries in many ways. These batteries exhibit the same voltage and current as their bulky counterparts, but their thinner dimensions allow for greater applications such as making thinner electronic devices, like cell phones, laptops and even implantable medical devices and reducing the weight of common devices that are run on battery power because of the batteries' high energy density. These batteries can be formed into any shape and they can be stacked, to be used in parallel, thus even further reducing the space needed for a battery, and figure (1-4) shows thin films ion battery. (Bates, J.B.,Dudney,et al 2000).

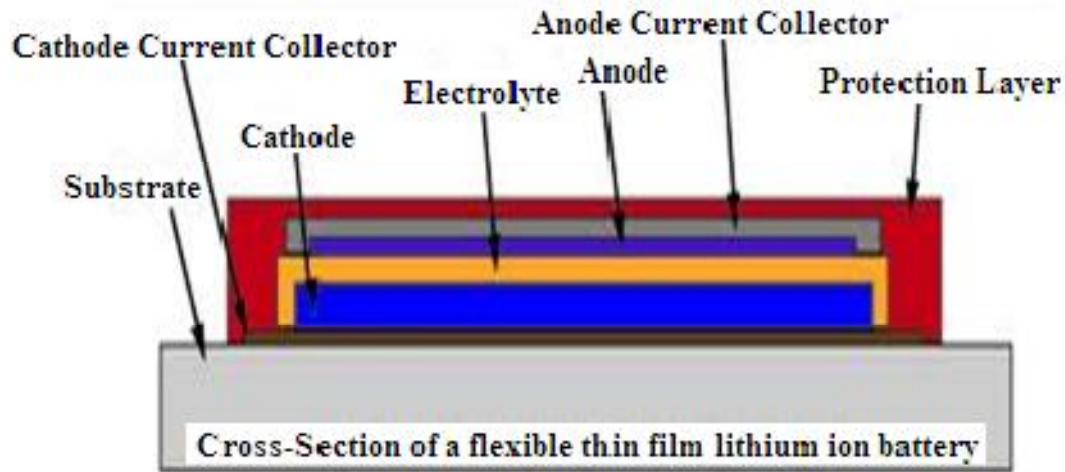


**Fig (1-4): Schematic representation of thin film lithium ion batteries**

### **1.6Types of Coating:**

All coatings- whether used for corrosion protection, to provide good aesthetics or a pleasing appearance, or for any other purpose will contain a film-forming material. This material may be organic or inorganic and, after application, may form a hard, impervious film, a soft porous film, or combinations in between. Furthermore, the filmforming material may be clear (unpigmented) or filled with a variety of different pigments, depending on its function. When the film-forming material (resin) contains pigments, it is called a binder. The binder will hold the pigment particles together and to the substrate over which it has been applied. When the binder (resin plus pigment) is dissolved in a solvent to make it liquid, the combination (solvent, binder, and pigment) is considered to be a vehicle. The term vehicle comes from the ability to transport and apply the liquid to the surface being coated. Once on the surface, the solvent evaporates and the vehicle becomes a pigmentbinder system. Application properties of the paint usually are characterized by the vehicle in a liquid condition. The viscosity, rate of solvent evaporation, and consistency of the wet coating are most important during application. After application, the pigments determine the corrosion-inhibitive properties and, generally, the color and some flow control properties of the applied coating. The binder determines the weatherability of the coating, its environmental

resistance, and the coating's ability to function in a given environment. The required surface preparation, and often the application equipment and techniques, are determined by the binder. The principal mechanisms by which binders form films are reaction with oxygen from the air (oxidation), evaporation of the solvent from the vehicle (solvent evaporation), or chemical crosslinking (polymerization). The coating film attained by these mechanisms can be either thermoplastic or thermosetting. Thermoplastic materials deform and soften on exposure to heat. Thermoset materials do not deform and remain hard upon heat exposure. Coating binders can be subcategorized according to the mechanism described above. However, with both oxidation and most polymerization film-forming mechanisms, solvent evaporation occurs initially, followed by a subsequent chemical reaction consisting of either a reaction with oxygen or chemical crosslinking. (Aad, G., Abbott, B., et al 2012). Solvent evaporative coatings also are called thermoplastics because, when heated, they become plastic and can soften and deform. Oxidation and chemically crosslinked coatings “set” and harden when cured; they do not soften or deform on heating and, therefore, are called thermosets. After application, most coatings “dry” by solvent evaporation to form a film that feels dry to the touch. However, the dried coating may not be cured, and additional chemical reactions may be required. Oxidation coatings require crosslinking with oxygen from the air, and polymerization coatings require a crosslinking chemical reaction between two or more coreactants to attain their final physical and chemical properties. Thermoset coating types dry and ultimately crosslink by reaction with oxygen from the atmosphere. All such coatings in this class contain drying oils that consist mainly of polyunsaturated fatty acids. The drying oil frequently is combined with a resin, usually by cooking or heating, to enhance water and chemical resistance. The curing reaction is accelerated by the presence of metallic salts as driers. After application, the coating dries by solvent evaporation. However, to attain maximum chemical and moisture-resistance

properties, the oil must react with oxygen from the air to crosslink, cure, and further harden. The auto-oxidation reaction occurs at a relatively fast rate shortly after application of the wet paint; and it continues throughout the life of the coating, although at a much slower rate. For most oil-based coatings, suitable moisture and chemical resistance occur within a few days after application, although maximum resistances may not be obtained until months or years after application. In time (often 20 or 30 years later), the oxidation reaction and continued drying of the oleoresinous binder system leads to cracking, embrittlement, and deterioration of the coating film. (Aad, G., Abbott, B., et al 2012).

Thin films are classified in many ways, mainly, according to the materials used for the coatings, the damage threshold, the strength and characteristics. There are metallic coatings and dielectric coatings. The metallic coatings always have lot of absorption and have only limited applications. The dielectric coatings have practically negligible level of absorption, and hence are very useful for various applications in optics (laser system, and imaging instruments). Higher laser damage threshold coatings are useful for high power lasers. The coatings with higher mechanical strength and higher abrasion resistance are used for mechanical tools increasing their life. (Kamal Nain Chopra. 2010).

### **1.7 Properties of thin films:**

To make sure that coatings which were produced by a given process satisfy the specified technological demands a wide field of characterization, measurement and testing methods are available. The physical properties of a thin film are highly dependent on their thickness. The determination of the film thickness and of the deposition rate, therefore, is a fundamental task in thin film technology. In many applications it is necessary to have a good knowledge about the current film thickness even during the deposition process, as e. g. in the case of optical coatings. Therefore one distinguishes between thickness measurement methods



which are applied during deposition ("in situ") and methods by which the thickness can be determined after finishing a coating run ("ex situ").(Davis, Peter L. et al 2015).Oregain increasing importance. Nonetheless, the desired mechanical, optical chemical or electronic properties are often opposed to the bulk properties which may be high mechanical stability, easy manufacturing or low material cost. Because of this fact a multitude of high tech components are composite materials which means that the surface properties significantly differ from the bulk properties. An example may be a mechanical part which has to exhibit high hardness (i. e. low wear under tribological load) as well as high fracture toughness (i. e. high resistance against crack propagation). One material alone may not fulfill these demands. The solution of the problem can be a composite material consisting of a surface zone (coating) with high surface hardness and a tough bulk core. Other machine components as e. g. high temperature blades of gas turbines have to exhibit high temperature and corrosion resistance as well as high mechanical stability. Also in this case one property such as corrosion resistance can be provided by a modified surface or a coating while mechanical stability is given by the base material. Another large field of examples is constituted by thin film systems which act as laser mirrors, anti reflex coatings and other optically active surface modifications. In the optical industry they are deposited on substrates which guarantee mechanical stability and other specific properties. Thin films can also be found in optoelectronic, electronic and magnetic components which can only be manufactured because of the special physical properties of thin films which may deviate significantly from those of the bulk material. A prominent example for this case are hard disk read heads based on the Giant Magneto resistance effect (GMR) which only operate due to the special properties of a combination of magnetic and insulating thin films.(Daniel Magnfalt. 2014).

### **1.7.1 Physical Properties of thin films:**

The emergence of thin film nanoscience as an identifiable field of investigation parallels the development and adaptation of surface structural and chemical probes to provide in situ real-time atomic-scale data during film growth. The next step in this evolutionary process, which evolving right now, is the addition of theory and modeling as standard approaches, used in combination with the above physical tools, to complement, design, and analyze experiments. The beautifully hierarchical complexity associated with thin film micro-nanostructure and surface morphological evolution, which arises from a diverse set of competitive kinetic instabilities operating on very different time and length scales, assures that thin film nanoscience and technology will remain a vital and exciting field long into the future.

One may obtain a wide variety of different surface/interface morphologies and film microstructure which are inherently related to dynamic growth mechanisms. (P.Meakin,Fractals,et al. 1998). These, in turn, have a significant and generally different influence on physical properties. Although epitaxial growth of a film in the layer-by-layer mode can commence in some cases within a certain temperature regime, such a growth mode may not always occur and instead growth front can be rough in the form of mounds (multilayer step structure; unstable growth) or due to noise induced roughening during the growth can lead to the formation of self-affine fractal morphologies. Besides kinetic effects during growth, stress relaxation in between film interfaces strongly alters growth characteristics and has to be taken certainly into consideration. (Hamblin, Michael R, Alberto.2015).

### **1.7.2 Magneto-transport (spin-polarized) properties:**

Systematic studies in spin polarised electron transport in magnetic multilayers which show giant magneto-resistance (GMR) effect, indicated that interface roughness as well as bulk impurities strongly influence the magnitude of the effect in a way that depends on the spin asymmetry for bulk and interfacial electron

scattering.(Brownlee, MD, M., 1995). Since the magnitude of the GMR effect is linked to the interface topology via the exchange coupling in magnetic multilayers, the interface quality is of crucial importance for magneto-electronic devices. Besides interface roughness, the presence of magnetic pin holes, that cause ferromagnetic alignment of parts of the sample, as well as precursors of these in the form of large spacer film fluctuations (which lead also to partial ferromagnetic alignment) reduce GMR. In addition, the presence of interface roughness in GMR multilayers can mediate 90 coupling, which can lead to perpendicular alignment of the magnetic moments of adjacent magnetic films at zero field, instead of an anti-parallel or parallel one, and thus reducing significantly GMR.(Magnfält, D., 2014).

### **1.7.3 Magnetic properties:**

Besides magneto-transport, the amount of disorder at the surface/interface can also influences magnetic properties of thin magnetic films, like for instance coercivity, magnetic domain structure, and magnetization reversal. (Martin, J.I., Nogues, J., et al 2003). These magnetic properties are important in

applications related to magnetic recording industry, magnetic memories, etc. By use of x-ray resonant magnetic scattering, the hysteretic behavior of CoFe thin films with varying roughness was investigated, and it was found that the coercivity increases with increasing surface roughness. For thin Co films deposited on plasma etched Si, the uniaxial magnetic anisotropy has been to decrease with increasing surface roughness. The coactivity increases with increasing surface roughness also for ultra-thin Co films on Ar+ sputtered Cu substrates. Finally, surface/interface roughness has been shown to have a significant influence on the demagnetizing field. (J.Pingliu, Eric Fullerton, OliverGutfleisch.2007).

### **1.7.4Electrical transport properties:**

Rough surfaces/interfaces of thin films contribute to electron scattering and thus to the film electrical conductivity. Oscillations in electrical resistivity vs thickness

(quantum size effects: QSE) have been observed i.e., in thin films, of Ag or Au. (Lucia Claudio Andreani, Angelo Bozzola, Piotr Kowalczewski, et al. 2014). The conductivity of epitaxial Ag/Si films was shown to be proportional to the square of the interface roughness amplitude and to have a complex dependence on the lateral roughness correlation length. For quantum wells, it has been shown that the mobility of the two-dimensional electrons in AlAs/GaAs quantum wells is strongly influenced by interface roughness. Roughness was also shown to have an influence on the Hall mobility of metal oxide-semiconductor (MOS) field effect transistor devices, and on the electron mobility of high-mobility Si inversion layers - which improves if the exponential correlation function at the Si/SiO<sub>2</sub> interface is taken into account. The interface roughness has also been shown to affect the electron sub-band structure of InAs/GaSb semiconducting quantum wells. Moreover, the degree of roughness irregularity at short lateral length scales has significant influence on the conductivity of metallic/semiconducting thin films. Nonetheless, additional complexity of the transport properties arises due to electron scattering by grain boundaries, in addition to scattering from surface/interface roughness. (Lucia Claudio Andreani, Angelo Bozzola, Piotr Kowalczewski, et al. 2014).

Surface resistivity could be defined as the material's inherent surface resistance to current flow multiplied by that ratio of specimen surface dimensions (width of electrodes divided by the distance between electrodes) which transforms the measured resistance to that obtained if the electrodes had formed the opposite sides of a square. In other words, it is a measure of the material's surface inherent resistance to current flow. Surface resistivity does not depend on the physical dimensions of the material. According to Ohm's law for circuit theory, the resistance of a material is the applied voltage divided by the current drawn across the material across two electrodes.

$$R = \frac{V}{I} \quad (1.1)$$

Where: R is Resistance (ohms), V is Voltage (volts) and I is Current (amperes).

This electrical resistance is proportional to the sample's length and the resistivity and inversely proportional to the sample's cross sectional area.

$$R = \rho \frac{L}{A} \quad (1.2)$$

Where:  $\rho$  = Resistivity, A = cross-sectional area, L = length.

(Maria P. Gutierrez, Haiyong Li, Seffrey Patton. 2002).

Thin films of semiconductors and insulators; metals do not have band gap. Why band gaps occur?. Basically, the interatomic distance in a material determines its band gap. In crystalline materials it is the lattice parameter. Any factor which influences the interatomic distance in a material can cause band gap shifts, eg. temperature, pressure, strain, concentration of impurities. (Milton Ohring. 2001).

### **1.7.5 Mechanical properties:**

Dynamic Mechanical Analysis (DMA) is a technique used to investigate the stiffness of materials as a function of temperature, humidity, dissolution media or frequency. A mechanical stress is applied to the sample and the resultant strain is measured by the instrument.

The problem of how surface influence the adhesion between elastic solids and a hard solid substrate is important from both the fundamental and technological point of view as for example in polymer/metal junctions. This topic was studied initially by Fuller and Tabor. And it was shown that a relatively small surface can remove the adhesion. In their model it was considered a Gaussian distribution of asperity heights with all asperities having the same radius of curvature. The contact force was obtained by applying the contact theory by Johnson et al. to each individual asperity. (D.M. Price. 2002). However, this approach considers surface over a single lateral length scale. The maximum pull-off force is expressed as a function of a single parameter which determines (the statistically averaged) competition between compressive forces from higher asperities that try to pull the

surfaces apart, and the adhesive forces from lower asperities that try to hold the surfaces together. On the other hand, random surfaces, which are commonly encountered for solid substrate surfaces, possess over many different length scales rather than a single one. In this case for random self-affine surfaces. (Daniel Magnfalt. 2014 and P. Meakin, Fractals, et al 1998). It has been shown that when the local fractal dimension  $D$  is larger than 2.5, the adhesive force may vanish or at least be reduced significantly. At any rate, for real polymers viscous-elastic effects are present which alter the interaction between polymer-metal substrate. In this case modifications are required since surface introduces fluctuating forces with a wide distribution of frequencies. (Daniel Magnfalt. 2014 and P. Meakin, Fractals, et al. 1998). Notably, the determination of the real contact area is a fundamental problem with important technological implications. The latter include, for example, heat transfer phenomena between solid bodies, electrical transport, sliding friction, adhesive forces between solid bodies in direct contact. (Paul Meakin. 2011).

The elastic moduli shouldn't be all that different - they are coming from the atom-atom bonds which are the same in the bulk and in thin films. Only if the number of atoms at or close to the surface is comparable to the total number of atoms in thin film, may need to think twice about this. In other words: only if consider thin to be in the order of atomic dimensions, bonding situation is so severely disturbed that you might find large differences between bulk and thin films elastic moduli. Parameters of plastic deformation like the critical yield strength (or hardness) can be far larger than bulk values. The reasons for this depend on many things (not least on the type of film), but if look at what determines the critical yield strength in bulk crystals, will find intrinsic length scales like the dislocation density (always ties up with some average distance between dislocations) or the grain size comparable to the total number of atoms in thin film, may need to think twice about this. In other words: only if consider thin to be in the order of atomic dimensions,

bonding situation is so severely disturbed that you might find large differences between bulk and thin films elastic moduli. Parameters of plastic deformation like the critical yield strength (or hardness) can be far larger than bulk values. The reasons for this depend on many things (not least on the type of film), but if you look at what determines the critical yield strength in bulk crystals, you will find intrinsic length scales like the dislocation density (always tied up with some average distance between dislocations) or the grain size. In thin film the grain size is one of the parameters. Parameters of plastic deformation like the critical yield strength (or hardness) can be far larger than bulk values. (Michael Depaz.2007).

The mechanical properties are:

(i) Stress: All coatings are in a state of more or less pronounced internal stress which is composed of two components, thermal stress and intrinsic stress,

The thermal stress is caused by different Coefficients of Thermal Expansion (CTS) of the coating and the substrate.

The thermal stress can, in principle, be calculated as opposed to the Intrinsic stress.

(ii) Adhesion: For all applications of coated materials sufficient adhesion regarding the respective application is paramount to guarantee a reasonable lifetime of the coated part. Adhesion is a macroscopic property which depends on the interatomic forces within the interface between substrate and film, on the internal stresses and on the specific load the coating is subjected to. The latter can be mechanical (pulling or shearing), thermal (high or low temperatures or thermal cycling), chemical (corrosion, either chemical or electrochemical) and can also result from other effects. According to Mattox a "good adhesion" is generally reached if:

1. A strong atom-atom bonding exists within the interface zone,
2. Low internal stresses exist within the film.
3. No easy mode of deformation or fracture exists.

4.No long term degradation is present in the composite substrate/coating.

The adhesion depends primarily on the choice of the partners present in the Composite, on the interface type, on the microstructure (and therefore on the deposition parameters of the coating) and on the pre treatment of the substrate. In the following these dependences shall be discussed with a special focus on PVD coating methods.

(iii) Hardness:A method for hardness measurement and evaluation of thin films on the material surface was proposed. Firstly, it is studied how to obtain the force-indentation response with a finite element method when the indentation is less than 100 nanometers, in which current nanoindentation experiments have not reliable accuracy. The whole hardness-indentation curve and fitted equation were obtained. At last, a formula to predict the hardness of the thin film on the material surface was derived and favorably compared with experiments.( Lin-dong WANG,MinLI,Tai-huaZHANG,et al.2003).

### **1.7. 6 Wetting phenomena:**

The phenomenon of wetting of solid substrates exposed to a gas (under thermodynamic equilibrium conditions) is a topic of intense research from both the fundamental and application point of view. (E.L.Grove, A.J Perkins. 1971 and Hamblin, Michael R, Alberto. 2015). The wetting of a substrate by a liquid is driven by the strong substrate/particle (van der Waals) attraction forces. Currently there is a rather clear microscopic understanding of wetting on flat solid substrates. (G.M.E.A.Backx. 2003). In this case, the liquid film thickness is described as a function of substrate/particle and inter-particle interactions for specified thermodynamic parameters (pressure and temperature). Experiments using noble gases on different substrates confirmed that the thickness of the wetting layer grows with increasing substrate/particle attraction (for fixed thermodynamic parameters), as well as that complete wetting(diverging liquid film thickness) occurs for stronger substrate/particle attraction than inter-particle



interactions (and thermodynamic conditions approaching liquid-gas coexistence). The presence of surface roughness and/or chemical heterogeneities further complicate wetting phenomena. (Daniel Bonn, Jems Eggers, Joseph Indekeu, Jacques. 2009).

### **1.7.7 The Optical properties:**

Electro-optical systems are intended for the transfer and transformation of radiant energy. They consist of active and passive elements and sub-systems. In active elements, like radiation sources and radiation sensors, conversion of energy takes place (radiant energy is converted into electrical energy and vice versa, chemical energy is converted in radiation and vice versa, etc.). Passive elements (like mirrors, lenses, prisms, etc.) do not convert energy, but affect the spatial distribution of radiation. Passive elements of electro-optical systems are frequently termed optical systems.

Following this terminology, an optical system itself does not perform any transformation of radiation into other kinds of energy, but is aimed primarily at changing the spatial distribution of radiant energy propagated in space. Sometimes only concentration of radiation somewhere in space is required (like in the systems for medical treatment of tissues or systems for material processing of fabricated parts).

In other cases the ability of optics to create light distribution similar in some way to the light intensity profile of an “object” is exploited. Such a procedure is called Imaging and the corresponding optical system is addressed as an imaging optical System. Of all the passive optical elements (prisms, mirrors, filters, lenses, etc.) lenses are usually our main concerns. It is lenses that allow one to concentrate optical energy or to get a specific distribution of light energy at different points in space (in other words, to create an “image”). (Naftaly Menn. 2004).

### **1.8 Technology of thin films deposition:**

The technology of thin film deposition has advanced dramatically during the past 30 years. This advancement was driven primarily by the need for new products and devices in the electronics and optical industries. The rapid progress in solid-state electronic devices would not have been possible without the development of new thin film deposition processes, improved film characteristics and superior film qualities. Thin film deposition technology is still undergoing rapid changes which will lead to even more complex and advanced electronic devices in the future. The economic impact of this technology can best be characterized by the worldwide sales of semiconductor devices. Technological progress of modern society depends on the material science and engineering community's ability to conceive the novel materials with extraordinary combination of physical and mechanical properties. (KrishnaSeshon. 2002).

There are many dozens of deposition technologies for material formation. Since the concern here is with thin-film deposition methods for forming layers in the thickness range of a few nanometers to about ten micrometers, the task of classifying the technologies is made simpler by limiting the number of technologies to be considered.

Basically, thin-film deposition technologies are either purely physical, such as evaporative methods, or purely chemical, such as gas- and liquid-phase chemical processes. A considerable number of processes that are based on glow discharges and reactive sputtering combine both physical and chemical reactions; these overlapping processes can be categorized as physical-chemical methods.

A classification scheme is presented in Table 1 where we have grouped thin-film deposition technologies according to evaporative glow discharge, gas-phase chemical, and liquid-phase chemical processes. The respective pertinent chapter numbers in this book have also been indicated.

Certain film formation processes such as oxidation, which, strictly speaking, are not deposition processes, have been included because of their great importance in solid-state technology, (KrishnaSeshan.2002).

## **CHAPTER TWO**

### **Multilayers thin films coating**

#### **2. 1 Introduction:**

Multilayers thin films coating have been extensively used for reflectivity modulation in various optical and optoelectronic components. These include anti-reflection (AR) and high-reflection (HR) coatings. Anti-reflection coating on lenses of cameras and telescopes, and fabrication of polarizing beam splitters and various optical filters and other components. The multilayer optical coating usually consists of a stack of several layers of non-absorbing dielectric materials with different refractive indices. The reflectance of such a film depends on the constructive or destructive interference of light reflected at successive boundaries of different layers of the multilayer stack. So, the choice of an appropriate sequence of these layers with suitable dielectric materials and their thicknesses that best satisfy the desired spectral response for the application is a crucial issue. Thus, to design the multilayer dielectric thin films and to optimize their coating conditions, a reflectivity and absorption spectrum simulation of these optical thin films is an essential tool, in films and multilayers are widely used in technology,

and their mechanical performance under severe environmental conditions often dictates design. Examples include electronic packages, coatings for thermal, chemical or abrasion protection, and ferroelectric actuators. (John W.Hutchinson, 1996).

## **2. 2 Deposition techniques for thin films:**

Deposition methods of thin films can be divided into two major categories:(i) Physical deposition processes. (ii) Chemical deposition processes. Several techniques have been developed (depending on the desired film properties) for the deposition of the thin films of the metal, alloys, semiconductors, ceramic, polymer and superconductors on a variety of the substrate material. The properties of thin films are extremely sensitive to the method of preparation. Underlying the performance and economics of thin film components are the manufacturing techniques that are used to produce the devices. Each method has its own merits and demerits and of course no one technique can deposit the thin films covering all the desired aspects such as cost of equipments, deposition conditions and nature of the substrate material. The vast varieties of thin film materials, their deposition, processing, fabrication techniques, spectroscopic characterization, optical characterization probes, physical properties and structure-property relationships are the key features of such devices and basis of thin film technologies. Physical methods cover the deposition techniques which depend on the evaporation or ejection of the material from a source that is evaporated or sputtered. Whereas chemical methods depend on specific reaction conditions like temperature, pH, concentration of precursors etc.. The chemical reactions may also depend on thermal effects as in vapour phase deposition and thermal growth. However, in all these cases a definite chemical reaction is required to obtain the final film. When one seeks to classify deposition of films by chemical methods, one finds that are available, into two more classes. The first of these classes is concerned with the chemical formation of the film from medium e.g. electroplating, chemical

reduction plating and vapour phase deposition. A second class is that of formation of this film from the precursor ingredients e.g. anodization, gaseous anodization, thermal growth, sputtering ion beam implantation, chemical vapor deposition (CVD), metal organo-chemical vapor deposition (MOCVD) and vacuum evaporation. The methods summarized under the classifications given are often capable of producing films defined as thin films i.e. 1  $\mu\text{m}$  or less and films defined as thick films i.e. 1  $\mu\text{m}$  or more. However, there are certain techniques which are only capable of producing thick films and these include screenprinting, glazing, electrophoretic deposition, flame spraying and painting. (Krishna Seshan, 2002).

The ability to deposit thin films of various materials is important for the fabrication of modern microelectronic devices and for enabling a variety of investigations of fundamental physical principles. There are many techniques for controllably depositing thin films onto a substrate with thicknesses as small as a few nm. Nanoparticles are commonly defined as particles less than 100 nm in diameter. Due to this small size, nanoparticles have a high surface-to-volume ratio. This increases the surface energy compared to the bulk material. The high surface-to-volume ratio and size effects (Quantum effects) give nanoparticles different chemical, electronic, optical, magnetic and mechanical properties from those of the bulk material. (Sudheerkumar, Ramana Rao, 2013).

### **2.2.1 Physical techniques**

There are two types of physical techniques:

#### **2.2.1.1 Physical Vapor Deposition (PVD)**

PVD processes proceed along the following sequence of steps:

- a) The solid material to be deposited is physically converted to vapour phase;
- b) The vapour phase is transported across a region of reduced pressure from the source to the substrate;

c) The vapour condenses on the substrate to form the thin film. The conversion from solid to vapour phase is done through physical dislodgement of surface atoms by addition of heat in evaporation deposition or by momentum transfer in sputter deposition. The third category of PVD technique is the group of so called augmented energy techniques including ion, plasma or laser assisted depositions.

#### **2.2.1.2 Evaporation technique:**

Evaporation or sublimation techniques are widely used for the preparation of thin layers. A very large number of materials can be evaporated and, if the evaporation is undertaken in vacuum system, the evaporation temperature will be very considerably reduced, the amount of impurities in the growing layer will be minimised. In order to evaporate materials in a vacuum, a vapor source is required that will support the evaporate and supply the heat of vaporization while allowing the charge of evaporate to reach a temperature sufficiently high to produce the desire vapour pressure, and hence rate of evaporation, without reacting chemically with the evaporate. To avoid contamination of the evaporant and hence of growing film, the support material itself must have a negligible vapour pressure and dissociation temperature of the operating temperature. (J.A. Dobrowolski .1995 and H.Pulker, J. 1987).

#### **Electron Beam Heating Evaporation**

This technique is based on the heat produced by high energy electron beam bombardment on the material to be deposited. The electron beam is generated by an electron gun, which uses the thermionic emission of electrons produced by an incandescent filament (cathode). Emitted electrons are accelerated towards an anode by a high difference of potential(kilovolts). The crucible itself or a near perforated disc can act as the anode. A magnetic field is often applied to bend the electron trajectory, allowing the electron gun to be positioned below the evaporation line(GSudheerKumer,Jagirdar,et al,2013).

#### **2.2.1.3 Sputtering technique:**

If a surface of target material is bombarded with energetic particles, it is possible to cause ejection of the surface atom: this is the process known as sputtering. The ejected atoms can be condensed on to a substrate to form a thin film. In sputtering there are two means of operation: dc and ac (radiofrequency), which also function in two configurations: magnetron dc (balanced and unbalanced) and magnetron ac (balanced and unbalanced). In dc discharge, the cathode electrode is the sputtering target and the substrate is placed on the anode, which is often at ground potential. The applied potential appears across a region very near the cathode, and the plasma generation region is near the cathode surface. The cathode in dc discharge must be an electrical conductor, since an insulating surface will develop a surface charge that will prevent ion bombardment of the surface. This condition implies that dc sputtering must be used to sputter simple electrically conductive materials such as metals, although the process is rather slow and expensive compared to vacuum deposition. An advantage of dc sputtering is that the plasma can be established uniformly over a large area, so that a solid large-area vaporization source can be established. On the other hand, in dc sputtering the electrons that are ejected from the cathode are accelerated away from the cathode and are not efficiently used for sustaining the discharge. To avoid this effect, a magnetic field is added to the dc sputtering system that can deflect the electrons to near the target surface, and with appropriate arrangement of the magnets, the electrons can be made to circulate on a closed path on the target surface. This high current of electrons creates high-density plasma, from which ions can be extracted to sputter the target material, producing a magnetron sputter configuration. A disadvantage of the magnetron sputtering configuration is that the plasma is confined near the cathode and is not available to active reactive gases in the plasma near the substrate for reactive sputter deposition. (C.H.S. Dupuy. AWCACHARD, 1974).

This method has various advantages over normal evaporation techniques in which no container contamination will occur. It is also possible to deposit alloy films

which retain the composition of the parent target material. Figure (2-1) shows the sputtering system.

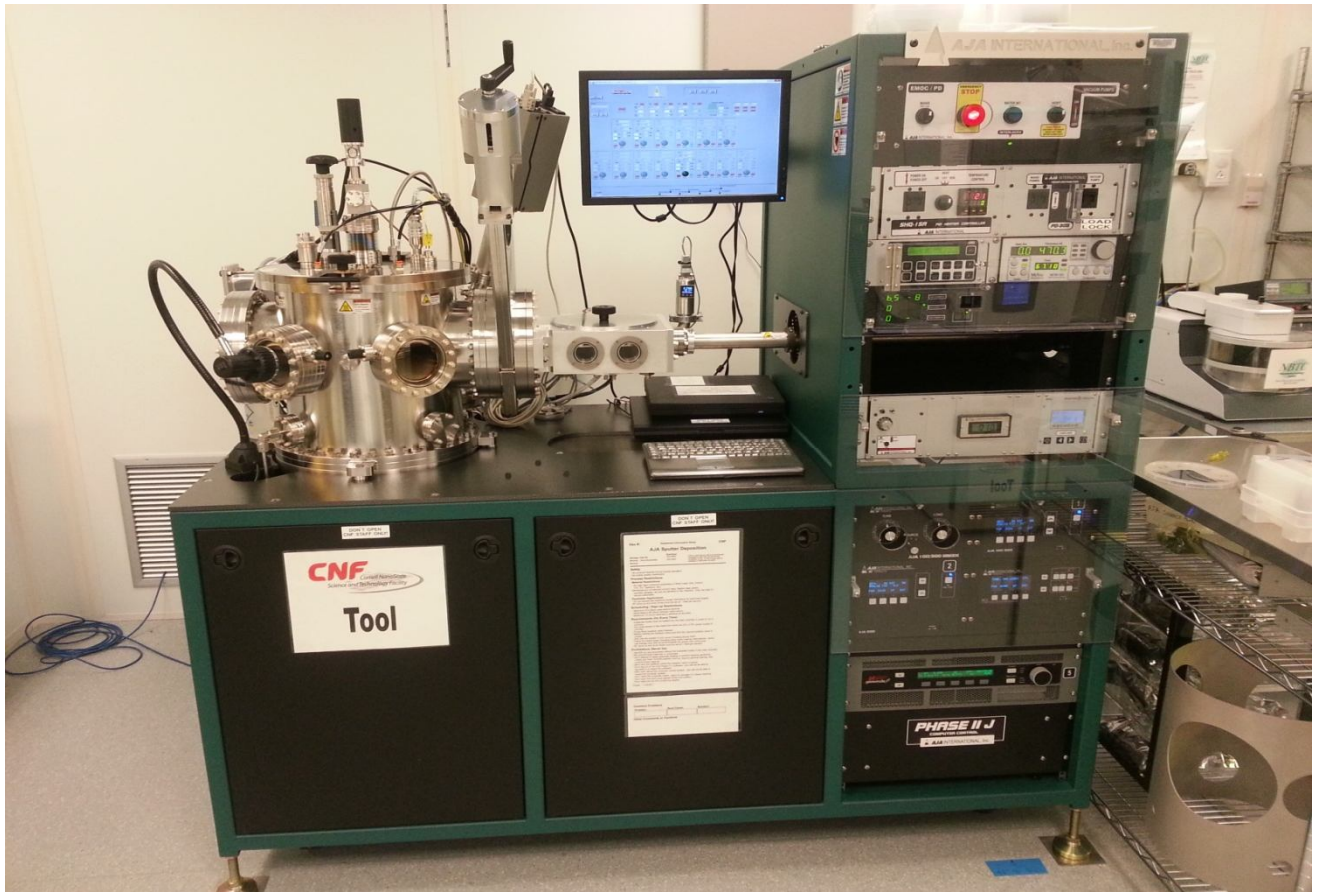


**Figure (2-1):The sputtering system.**

#### **2.2.1.4 Ion plating technique:**

In this atomistic, essentially sputter-deposition process, the substrate is subjected to a flux of high energy ions, sufficient to cause appreciable sputtering before and during film deposition. The advantages of physical methods are laid in dry processing, high purity and cleanliness, compatibility with semiconductor integrated circuit processing and epitaxial film growth. However, there are certain disadvantages such as slow deposition rates, difficult stoichiometry control, high temperature post deposition annealing often required for crystallization and high capital expenditure. Ion plating used a thermal vaporization source or a chemical



vapor precursor or a combination of the two sources. Later, when high-rate sputter vaporization sources were used as a source of deposited material, the process was called “sputter ion plating” by some authors and “bias sputtering” by others. In the ion plating process deposited material may be “back-sputtered” if the bombarding energies are above some “sputtering threshold” energy. Generally this threshold energy is 50 to 100 eV depending on the depositing material and mass of the bombarding species. Bombardment below this energy can modify film properties without having any “back sputtering”. Also at low bias potentials high ion fluxes are used to modify the properties of the coating. When deposition compound or alloy materials, preferential back-sputtering may affect the composition of the deposit. (Donald M. Mattex. 2003).

### **2.2.2 Chemical and electrochemical techniques:**

It is an electrochemical reaction, any process either caused or accompanied by the passage of an electric current and involving in most cases the transfer of electrons between two substances, one solid and other a liquid (Buttry, D.A. and Ward, M.D., 1992). The phenomenon of electrolysis is governed by the Faraday's laws, when a metal electrode is immersed in a solution containing ions of that metal, a dynamic equilibrium  $M \rightleftharpoons M^{n+} + n e^{-}$  (M- Metal atom &  $x = S, Se, Te$ ) is set up. The electrode gains a certain charge on itself which attracts oppositely charged ions & molecules holding them at electrode / electrolyte interface. A double layer consisting of an inner layer of water molecules interposed by preferentially adsorbed ions & outer layer of the charge opposite to that of the electrode is formed. During deposition ions reach the electrode surface, stabilize on it, release their ligands, release their charges and undergo electrochemical reaction. The rapid layer depletion of the depositing ions from the double layer is compensated by a continuous supply of fresh ions from the bulk of the electrolyte. The factors influencing the electro deposition process are current

density, bath composition, pH of the electrolyte, temperature of the bath, agitation and electrode shape. (Sunil Kumars, Shivani Pande, Prateek Verma, 2015).

### **2.3 Optical Coatings:**

An optical coating is one or more thin layers of material deposited on an optical component such as a lens or mirror, which alters the way in which the optic reflects and transmits light. One type of optical coating is an antireflection coating, which reduces unwanted reflections from surfaces, and is commonly used on spectacle and photographic lenses. Another type is the high-reflector coating which can be used to produce mirrors which reflect greater than 99.99% of the light which falls on them. Besides that, different filters for certain wavelengths are manufactured by optical coatings. More complex optical coatings exhibit high reflection over some range of wavelengths, and anti-reflection over another range, allowing the production of dichroic thin-film optical filters (Sunil Kumars, Shivani Pande, Prateek Verma, 2015).

Optical coatings are used to alter the reflectance, transmittance, absorbance, or polarizer properties of optical components. The optics being coated is usually called the substrate. The coating is deposited in high vacuum using the process of evaporation by either e-beam, resistive heat or IAD (Ion Assisted Deposition) in conjunction with an e-beam source. Coating materials include metal (Au, Al, Ag, Ni-Cr, Cr and so on), dielectrics (Oxides, Fluorides and Sulfides) and semiconductors (Si, Ge). Optical interference coatings respond differently to s and p polarized light. For this reason, it is essential to specify s, p, or random (the average of the s and p performance) polarization when the angle of incidence exceeds 20 degrees. (Mohammed, S.E.E., 2007).

### **2.4 General Theory of Filters:**

There are many ways of describing the performance of optical coatings and filters. For example, transmission and reflection filters intended for visual applications

are adequately described by a color name alone, or by reference to one of the several existing color systems. There also exist other specialized filter specifications for specific applications. However, the most complete information on the performance of a filter is provided by spectral transmittance, reflectance, absorptance, and optical density curves.

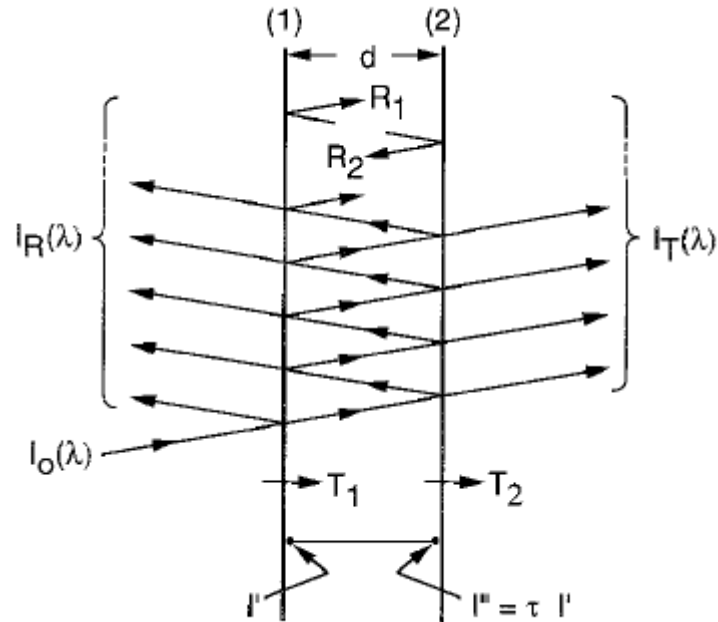


**Figure (2-2): Specular transmission and reflection of light by a plane-parallel plate.**

Referring to Figure 2.2, at a wavelength  $\lambda$ , the normal incidence spectral transmittance  $T(\lambda)$  of a filter placed between two semi-infinite media is equal to the ratio of the light intensity of that wavelength transmitted  $I_T(\lambda)$  by the filter to that incident  $I_0(\lambda)$  upon it ,

$$T(\lambda) = \frac{I_T(\lambda)}{I_0(\lambda)} \quad (2-1)$$

At nonnormal incidence, the component of the intensity perpendicular to the interface must be used in the preceding equation 2-2. The spectral reflectance  $R(\lambda)$  of a filter is defined in a similar way:

$$R(\lambda) = \frac{I_R(\lambda)}{I_0(\lambda)} \quad (2-2)$$

The relationship between the transmittance  $T(\lambda)$  and the density of a filter  $D(\lambda)$ , sometimes also called the absorbance, is given by

$$D(\lambda) = \log \frac{1}{T(\lambda)} \quad (2-3)$$

Transmittances and reflectances can be plotted using either linear or logarithmic scales. The logarithmic scale is particularly well suited whenever accurate information about the low-transmission or reflection region is to be conveyed. However, this is done at the expense of detail at the high end of the scale. Wavelengths are normally specified in micrometers ( $\mu\text{m}$ ) because this is the most convenient unit for the spectral range. In the following discussion, the dependence of the transmittance, reflectance, and absorbance on wavelength will be implicitly assumed. (Dobrowolski, J.A., 1995).

## **2.5 Transmission and Reflection of Coatings on a Substrate:**

Many multilayer coatings are deposited onto a transparent or partially transparent substrate. Both the multilayer and the substrate contribute to the overall performance of the filter. For example, absorption in the substrate is frequently used to limit the transmission range of the filter. Reflectances at the filter interfaces need also to be considered. However, they can be reduced by antireflection coatings, or by cementing several components together.

In general, a filter can consist of multilayer coatings deposited onto one or both sides of a substrate. The overall transmittance  $T_{\text{total}}$  of a filter can be expressed in terms of the internal, or intrinsic transmittance  $\tau$  of the substrate and the transmittances  $T_1$ ,  $T_2$  and internal reflectance's  $R_1$ ,  $R_2$  of each surface of the substrate (Fig. 2.2).

The internal transmittance  $\tau$  of a substrate is defined to be the ratio of the light intensity  $I''$  just before reaching the second interface to the intensity  $I'$  just after entering the substrate (Fig 2.2)

$$\tau = \frac{I''}{I'} \quad (2-4)$$

Providing that the incident light is not coherent, there will be no interference between the beams reflected from the two surfaces of a substrate, even when the surfaces are plane-parallel. A summation of all the partial reflections leads to the following expression for the overall spectral transmittance  $T_{total}$  of a filter:

$$T_{total} = \frac{T_1 T_2 \tau}{1 - R_1 R_2 \tau^2} \quad (2-5)$$

If all the materials in the filter are nonabsorbing, then.

$$T_{total} = \frac{T_1 T_2}{1 - R_1 R_2} \quad (2-6)$$

If  $R_1$  is small, an appropriate expression for  $T_{total}$  is

$$T_{total} \approx [1 - R_1 (1 - R_2)] T_2 \quad (2-7)$$

However, this last approximation is not valid in general; some infrared substrate materials have high reflection coefficients and in such cases Eq.(2-6) must be used.

## 2.6 Transmission Filters in Series and in Parallel:

To obtain a desired spectral transmittance, it is frequently necessary to combine several filters. One common approach is to place several filters in series (Fig. 2.3 a). Because of the many different partial reflections that may take place between the various surfaces, precise formulas for the resulting transmittance are complicated. (Dobrowolski, J.A., 1995).

Accurate calculations are best carried out using matrix methods. To a first approximation, the resultant transmittance  $T'$  of a filter system consisting of  $k$  individual filters placed in series is given by:

$$T' = T'_1 T'_2 T'_3 \dots T'_k \quad (2-8)$$

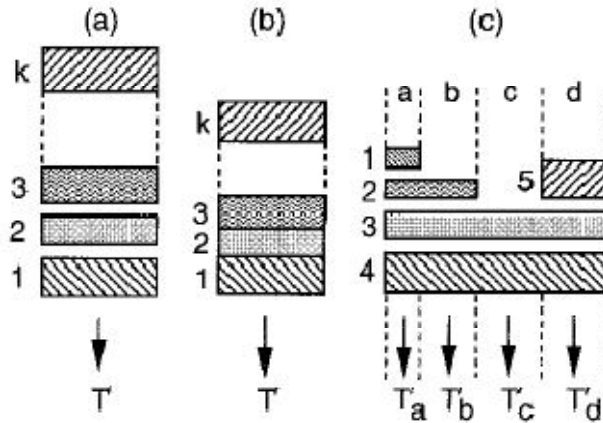


**Figure (2-3):** Transmission filters arranged in series and in parallel. The filters can be air-spaced (a) and (c) or cemented (b).

Here  $T'_i$  is the total transmittance of filter  $i$ . This expression is valid only if the reflectance's of the individual filters are small or if the interference filters are slightly inclined to one another and the optics are arranged in such a way that the  $T'_1$ ,  $T'_2$ ,  $R'_1$ , and  $R'_2$  detector sees only the direct beam.

Under other circumstances, the use of this expression with interference filters can lead to serious errors. Consider two separate filters placed in series and let correspond to the transmittances and reflectance's of the two filters. If  $T'_1 = T'_2 = R'_1 = R'_2 = 0.5$ , then according to Eq. (2-8), the resulting transmittance will be  $T_i$ . For this simple case the precise expression can be derived from Eq. (2-5) and is given by

$$T' = \frac{T_1 T_2'}{1 - R'_1 R'_2} \quad (2-9)$$

Evaluating this expression one obtains  $T_i$ . This is significantly different from the result obtained from the application of Eq. (2-8).

Some spectral transmittance curves cannot be easily designed by placing filters in series alone. For certain applications it is quite acceptable to place filters not only in series, but also in parallel. This introduces areas as additional design parameters. Thus, for example, the effective spectral transmittance  $T_i$  of the filter shown in Fig (2-3c) would be given by

$$T^I = \left( \frac{a}{A} T_a^I + \frac{b}{A} T_b^I + \frac{c}{A} T_c^I + \frac{d}{A} T_d^I \right) \quad (2-10)$$

Where:

A = overall area of filter.

a, b, c, d = areas of the four zones.

$T_a^I, T_b^I, T_c^I, T_d^I$  = transmittances of four zones.

The latter are given by

$$T_a^I = T_1^I \cdot T_2^I \cdot T_3^I \cdot T_4^I$$

$$T_b^I = T_1^I \cdot T_2^I \cdot T_3^I \quad (2-11)$$

$$T_c^I = T_1^I \cdot T_2^I$$

$$T_d^I = T_1^I \cdot T_2^I \cdot T_3^I \cdot T_5^I$$

Great care must be exercised when using such filters. Because the spectral transmittance of each zone of the filter is different, errors will result unless the incident radiation illuminates the filter uniformly. Similar care must be used when employing the filtered radiation. One way proposed to alleviate these problems is to break the filter down into a large number of small, regular elements and to reassemble it in the form of a mosaic.

## 2.7 Reflection Filters in Series:

If radiation is reflected from  $k$  different filters, the resultant reflectance  $R^I$  will be given by

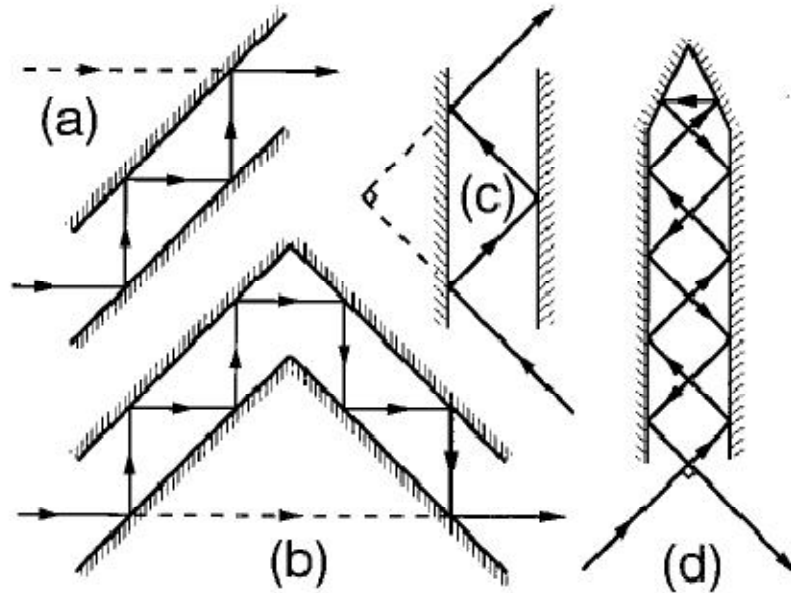
$$R^I = R_1^I \cdot R_2^I \cdot R_3^I \cdot \dots \cdot R_K^I \quad (2 - 12)$$

Which is analogous to Eq. (2-11) for the resultant transmittance of filters placed in series?

Many of the considerations of that section also apply here. For instance,  $R^I$  will be significant only at those wavelengths at which every one of the reflectors has a significant reflectance. Metal layers and thin-film interference coatings can be used exclusively or in combination.

For the sake of convenience the number of different reflecting surfaces used is normally restricted. The outlines of some possible reflector arrangements given in Fig (2.4) are self-explanatory. The arrangement shown in Fig (2.3 b) does not deviate or displace an incident parallel beam. The number of reflections depends in each case on the lengths of the plates and on the angle of incidence of the beam. Other arrangements are possible. (Dobrowolski, J.A., 1995).





**Figure(2-4): Various arrangements for multiple reflection filters.**

Clearly, reflection filters placed in series require more space and are more complicated to use than transmission filters.

A thin-film designer may be asked to design a multilayer coating in which the transmittance, reflectance, and / or absorptance values are specified at a number of wavelengths, angles, and polarizations of the incident light. The designer may be required to provide a coating with many other more complicated properties, including integral quantities such as CIE color coordinates, solar absorptance, or emissivity. The parameters that can be used to reach these goals are the number of layers in the multilayer, the layer thicknesses, and the refractive indices and extinction coefficients of the individual layers and of the surrounding media. Clearly, the more demanding the performance specifications, the more complex the resulting system. Many different methods have been developed for the design of multilayer coatings. (Dobrowolski, J.A., 1995).

## **2.8 Antireflection Coatings:**

Antireflection coatings were the principal objective of much of the early work in thin-film optics. Of all the possible applications, antireflection coatings have had

the greatest impact on technical optics, and even today, in sheer volume of production, they still exceed all other types of coating. In some applications, antireflection coatings are simply required for the reduction of surface reflection. In others, not only must surface reflection be reduced, but the transmittance must also be increased. The crown glass elements in a compound lens have a transmittance of only 96% per untreated surface, while the flint components can have a surface transmittance as low as 90%. The net transmittance of even a modest number of untreated elements in series can therefore be quite low. Additionally, part of the light reflected at the various surfaces eventually reaches the focal plane, where it appears as ghosts or as a veiling glare, thus reducing the contrast of the images. This is especially true of the zoom lenses used in television or photography, where 20 or more elements may be included, and which would be completely unusable without antireflection coatings.

Antireflection coatings can range from a simple single layer having virtually zero reflectance at just one wavelength, to a multilayer system of more than a dozen layers, having virtually zero reflectance over a range of several octaves. The type used in any particular application will depend on a variety of factors, including the substrate material, the wavelength region, the required performance, and the cost.

In the visible region, crown glass, which has a refractive index of around 1.52, is most commonly used. This presents a very different problem from infrared materials, which can have very much higher refractive indices. It is convenient, therefore, to split what follows into antireflection coatings for low-index substrates and antireflection coatings for high-index substrates, corresponding roughly to the visible and infrared. There is no systematic method for the design of antireflection coatings. Trial and error, assisted by approximate techniques backed up by accurate computer calculation, is frequently used. Very promising designs can be further improved by computer refinement. The vast majority of antireflection coatings are required for matching an optical element into air. Air has an index of

around 1.0003 at standard temperature and pressure, which, for practical purposes, can be considered as unity. The earliest antireflection coatings were on glass for use in the visible region of the spectrum. A single-layer antireflection coating on glass, for the center of the visible region, has a distinct magenta tinge when examined visually in reflection. (Kamal Nain Chopra, 2010).

## **2.9 Literature review:**

Several literature reports have indicated that thin film geometries of MnOx provides specific capacitances that are much higher than bulk MnOx powders. The good stability, cyclability and high specific capacitances of manganese oxide MnOx has recently promoted a growing interest in utilizing MnOx in asymmetric supercapacitor electrodes. Plasma enhanced chemical vapor deposition (PECVD) is a versatile technique for the production of metal oxide thin films with high purity and controllable thickness. The purity and oxidation state of the MnOx films were studied by Fourier transform infrared spectroscopy and X-ray photo electron spectroscopy. Preliminary electrochemical testing of MnOx films deposited on carbon fiber electrodes in aqueous electrolytes indicates that the PECVD synthesized films are electrochemically active (Anna R. et al, 2014).

Recently a developed ion beam layer removal method was used to determine the stress profile in a thin film system. The system consists of a thin tungsten and titanium nitride film deposited on a silicon substrate. The stresses are calculated from the deflection of a focused ion beam machined cantilever by means of Euler–bernoulli beam theory and finite element simulations coupled with optimizing algorithms, different boundary conditions in the thin film system is strongly manufacturing related variations in the cantilever geometry only slightly influence the stress distribution. (R. schongrundner, et al, 2014).

Deposition technology of Rhodamine dye dissolved by Chloroform was done with certain concentration, to produce one layer of thin film.

The deposition of the dye above was done and controlled the thickness by the He – Ne laser to move through the solution deposit on substrate (glass). The incident and transmitted laser intensity were measured, before and after deposition.

Ten samples of thin films were produced from the dyes above in room temperatures and with different temperatures. From their optical properties, some films can be used as filters and others as reflectors. (Suliman.E. M., 2007).

Thermal evaporation technique was used to deposit Nickel layer on silicon wafer & the deposited sample post annealed at different temperatures in vacuum and or different gas environments, and the sheet resistance of the films was measured using conventional four/two probe method with high surface to volume ratio and size effects. (G Sudheer Kumer, Jagirdar, et al, 2013).

## **CHAPTER THREE**

### **The experimental part**

#### **3-1 Introduction:**

The main purposes of this chapter are the description of the experimental setup used for the production of multilayers thin films, as well as the materials and the experimental procedure.

#### **3-2 The experimental setup:**

The schematic diagram of the setup is shown in figure (3-1), it was composed of the followings.

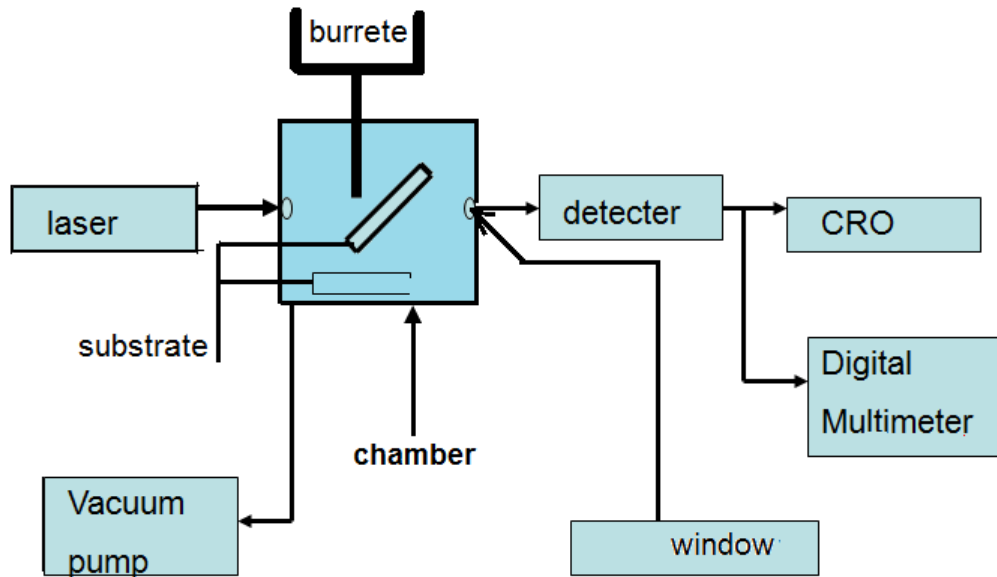


**Figure (3-1):Schematic diagram of the experiment setup.**

### **3-2-1The vacuum chamber:**

It is a sort of cubic box made of zinc material, its dimensions are:  $22 \times 22 \times 22 \text{ cm}^3$ .

The chamber contains two circular glass windows on the two parallel sides; the diameter of each is (0.5 cm). The first window is for laser input and the second is for the detector.

There is a circular cover, with a diameter of 8.5 cm on the upper side of the box. There is a small hole at the center of the cover with 0.3cm in diameter. The purpose of this hole is to allow insertion of a T-shape tube with two- connections via plastic channel. In the bottom of the chamber there are two holders within the chamber, one of them of an angle of 45 degrees and the other of a horizontal angle of 180 degree, and that are for the substrate used for the deposition of the thin films. There is also a small hole in the bottom side of the chamber connect it to the vacuum pump. This pump is connected with vacuum gauge to measure the pressure inside the chamber.

### **3-2-2 The vacuum pump:**

To create a vacuum in a system it is necessary to move most of the molecules of gas out of the system. The molecules will move only if there is a pressure difference between the two regions of the space (low and high pressure). The low region is a space with little number of molecules, while the high pressure region is a space with larger number of molecules.

Any device which can induce pressure difference between the two regions in the space is called a vacuum pump. Then the vacuum pump is a device for evacuating air out of a chamber. Figure (3-2) shows the vacuum pump which was used in this work, table (3-1) illustrate its specifications.

**Table (3-1):The specifications of the vacuum pump**

Model	PHYWE 0275.93
Pumping speed	$3.5 \text{ m}^3 \text{ h}^{-1}$
Ultimate vacuum	$1.5 \times 10^{-4} \text{ mbar}$
Origin	German



**Figure (3-2): A photograph of the vacuum pump.**

### 3-2-3 The vacuum gauge:

This gauge is a special device which measures the pressure in the chamber. The simplest mechanical gauge is a chamber divided by a membrane. One side of the chamber is connected to the vacuum container and the other to the known pressure tank (it can simply open, therefore it will be under the atmospheric pressure). The membrane is attached to the pointer mechanism. Depending on the membrane deformation, the pointer will show the vacuum level. A gauge like this is considered to be a coarse or rough gauge. This gauge is a device used for measuring pressure in the chamber during evacuation. Table (3-2) shows the specifications of the vacuum gauge used in this work.

**Table (3-2): The specifications of the vacuum gauge**

Model	Blazer Bg 519776- T
Type	TPG 031
Volt	230
VA	50- 60 c / s

The pressure gauge used in this work contains two ranges: the first is the "bar" gauge and the other is the "mbar" gauge, see figure (3-3).



**Figure (3-3): A photograph of the vacuum gauge.**

**3-2-4. The photodetector:**

The photodetector is a device converts the incident optical radiation into an electrical current or voltage which is proportional to the light intensity.

The detector used in this work was (FG and G), model (450-1), made in USA. Figure (3-4) shows a photograph of the detector.



**Figure (3-4): A photograph of the detector**

**3-2-5 The Burette:**

It is a glass-tube of 0.4 cm diameter, provided with a control valve for opening and closing the tube. It contains the liquid used for deposition.

**3-2-6 The digital oscilloscope (CRO):**

The digital oscilloscope used in this work was model (TDS200, 100 MHz), manufactured by Tektronix company, USA.

**3-2-7 The digital multimeter:**



The specifications of the digital multimeter used in this work was:

MY-64 Large LCD, 1000V, 10A.

### 3-2-8 The UV-1800 spectrophotometer:

This device was used to record the absorption spectrum of the solutions and the solvents. This device responds over the approximate spectral range of 190 to 1100nm. Figures (3-5) and (3-6), show photographs of the (UV-1800 spectrometer) made in Japan.



**Figure (3-5): A photograph of the spectrometer (UV-1800).**

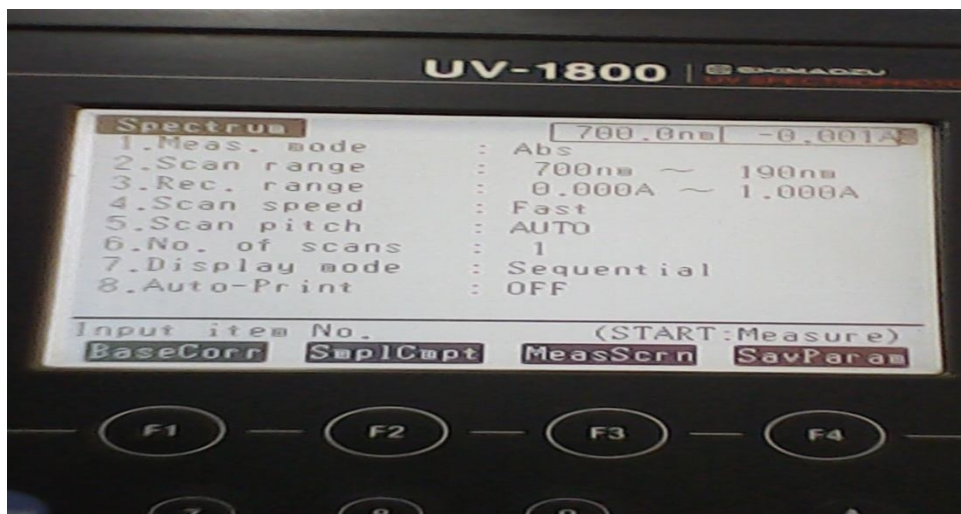


**Figure (3-6): A photograph of the screen of the spectrometer (UV-1800).**

### **3-3 The laser sources:**

Different laser sources were used to measure the thickness and to determine the optical properties of the deposited multilayers thin films. The lasers used in this study were:

#### **3-3-1 He-Ne laser:**

The most common and inexpensive laser, the helium-neon laser is usually constructed to operate in the red at 632.8 nm. It can also be constructed to produce laser action in the green at 543.5 nm and in the infrared at 1523nm. Helium-neon lasers are common in the introductory physics laboratories, but they can still be dangerous, where the unfocused 1 mW He-Ne laser has brightness equal to the sunshine on a clear day ( $0.1 \text{ Watt/cm}^2$ ). The helium gas in the laser tube provides the pumping medium to attain the necessary population inversion for laser action.

The Helium- neon laser used in this work was manufactured by PHYWE SYSTEM GmbH Company, Germany. It has 632.8 nm wavelength with 1 mW output power. Figure (3-7) shows a photograph of this device.



**Figure (3.7):A photograph of He – Ne laser.**

#### **3-3-2: Diode laser:**

Omega laser used in this work is a type of diode laser with three probes, the first with the wavelength of 675 nm, CW of output power 30 mW, and the second probe with wavelengths 820 nm, CW of output power 200 mW, and the third one with the wavelength 915 nm and output power 100 mW. It was manufactured by omega company-England. Figure (3-8) shows a photograph of this device.



**Figure (3-8):A photograph of omega laser xp system.**

### **3-3-3The Diode laser (532 nm):**

Diode laser with wavelength of 532 nm and 100mW output power was used in this work, it was made by (IouthLincs), manufactured in the UK.

### **3-3-4The red diode laser (671 nm):**

A red diode laser with 671 nm wavelength and 100 mW was used in this work. It was made by (Rothinar LaserTechnolikGmbh/Austria).

### **3-4 The materials:**

Different dyes were used as samples to fabricate multilayers thin films, they are:

#### **3-4-1Rhodamine 6G:**

Rhodamine is a family of related chemical compounds, fluorine dyes. Examples are Rhodamine 6G and Rhodamine B. They are used as dye and as dye laser gain medium.

Constitution: Benzoic Acid, Ethyl ester, mono hydrochloride Rhodamine  $590C_{28}H_{31}N_2O_3Cl$ . Figure (3-10) shows the chemical formula of Rhodamine 6G.

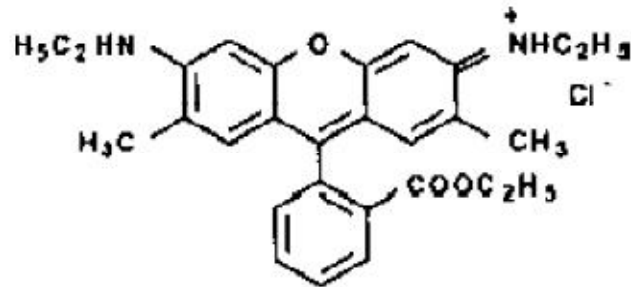


**Fig (3-9): The chemical formula of Rhodamine 6G.**

### 3-4-2 Phenexazon:

Constitution:

9-Diethylamino-5H-benzo (a) phenoxazin-5-one  $C_{20}H_{18}N_2O_2$ . Figure (3-11) shows the chemical formula of Phenexazon.

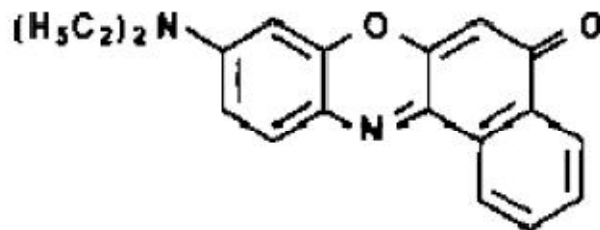
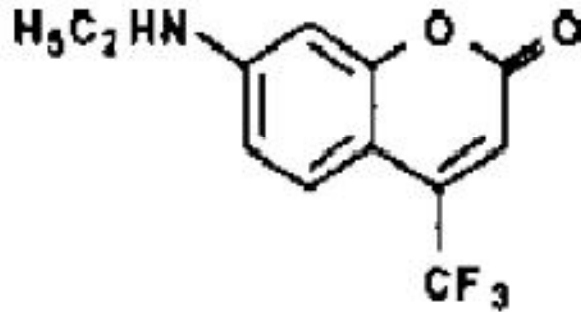


**Fig (3-10): The chemical formula of Phenexazon.**

### 3-4-3 Coumarin 500:

Constitution:  $C_{12}H_{10}NO_2F_3$ . Figure (4-11) shows the chemical formula of Coumarin 500.



**sFig (3-11):Thechemicalformula of Coumarin 500**

Figure (3-12) shows a photograph of the experimental setup used in this work to fabricate multilayersthin films.



**Figure (3-12): A photograph of the experimental setup**

1- Vacuum pump.

- 2- Vacuum gauge.
- 3- Laser source
- 4- Chamber
- 5- Burrete'
- 6- Digital multimeter.
- 7- CRO

### **3.5The Experiment Procedure:**

The experimental procedure for obtaining multilayers thin films was done as follows:

To prepare solution from Rhodamine 6G dye, the steps were:

- (1) 0.4 g of Rhodamine was dissolved in 10 ml of ethanol.
- (2) 1ml of the above solution was completed to 10ml by ethanol.
- (3) From the solution in (2), 1 ml was completed to 10 ml by ethanol.
- (4) From the solution in (3), 5 ml was completed to 10 ml by ethanol.
- (5) 1ml from the solution in (4) was completed to 10 ml by ethanol.
- (6) The solution in (5) was deposited on the substrate.

To prepare solution from Phenexazon dye, the steps were:

- (1) 0.3g of Phenexazon was dissolved in 10 ml by ethanol.
- (2) 1ml of the above solution was completed to 10 ml by ethanol.
- (3) From the solution in (2), 1 ml was completed to 10 ml ethanol.
- (4) Also from the solution in (3), 1 ml was completed to 10 ml by ethanol.

The solution in (4) was deposited on the substrate.

To prepare solution from Coumarin 500 dye. The steps were:

#### **3-5-1 The procedure of sample one:**

Sample one consists of three layers. The first layer composed of Phenexazon, the second is Rhodamine 6G, while the third one composed of Coumarin500. The thin film was prepared and characterized as follows:

(1) The setup was arranged as shown in figure (3-1).

(2) The solution was prepared by dissolving the dyes (Phenexazon, Rhodamine 6G, Coumarin 500) every one alone in the ethanol spirit for obtaining the lowest concentration, lowest absorption.

(3) The sample holder was inserted in the vacuum chamber, which was closed after that carefully.

(4) The vacuum pump was turned ON, then the air was evacuated from the chamber till the pressure reach  $0.3 \times 10^{-2}$  mbar.

(5) Helium –neon laser was turned ON, and then the incident laser intensity ( $I_0$ ) was measured by the digital multimeter, and the signal was detected by CRO.

(6) Phenexazon was put in one of the burette, and Rhodamine in the other. The valve of the first burette was open to deposit a layer from phenexazon, the laser signal was detected during the deposition, then the interference fringe was photographed, the deposition time was measured, it was eleven seconds for deposition of one layer with thickness equal half the He-Ne wavelength.

(7) The valve of the first burette was turned OFF.

(8) The valve of the second burette that contains the solution of Rhodamin was open to deposit a layer from Rhodamine 6G on the same substrate and the same above steps were repeated.

(9) Helium –neon laser was turned ON, and then the transmitted intensity ( $I$ ) was measured by the digital multimeter, and the signal was detected by CRO.

(10) For obtaining a layer of coumarin on the same substrate, the coumarin was put in the first burette and deposition was done within eleven seconds.

(11) The transmitted intensity of He-Ne laser ( $I$ ) was measured.

(12) Thickness of the thin film was controlled through the interference fringes. The thickness of each layer was half the wavelength of He-Ne (632.8nm), the thickness of this sample was  $(3/2 \lambda)$ , equal 949.2nm.

(13) The transmission spectrum of sample one was recorded in the region between (532-915 nm), by measuring ( $I_0$ ) and ( $I$ ) before and after deposition of the layers above.

(14) The transmission, reflection, absorption coefficient and the refractive index, for this sample were calculated.

### **3-5-2 The procedure of sample two:**

Sample two consists of three layers. The first layer composed of Phenexazon, the second was Rhodamine 6G, while the third one was composed of Coumarin500. This sample was prepared as follows:

(1) The chamber was opened through the upper cover for replacing the substrate with another and the burettes were cleaned by applying the ethanol spirit.

(2) The chamber was closed carefully.

(3) The vacuum pump was turned ON, then the air was evacuated from the chamber till the pressure reach  $0.3 \times 10^{-2}$  mbar.

(4) Phenexazon was put in one of the burettes, and Rhodamin in the other. The valve of the first burette was open to deposit a layer from phenexazon, the laser signal was detected during the deposition, then the interference fringes were



photographed, the deposition time was measured, it was eleven seconds for deposition of one layer with thickness equal half the He-Ne wavelength.

(5)The valve of the first burette was turned OFF.

(6)The valve of the second burette that contains the solution of Rhodamin was open to deposit a layer from Rhodamine 6G on the same substrate and the same above steps were repeated.

(7)Helium –neon laser was turned ON, and then the transmitted intensity (I) was measured by the digital multimeter, and the laser signal was detected by CRO.

(8) For obtaining a layer of Coumarin on the same substrate the Coumarin was put in the first burette and deposition was done, within twenty two seconds.

(9)Helium –neon laser was turned ON, and then the transmitted intensity (I) was measured by the digital multimeter, and the signal was detected by CRO.

(10) The transmitted intensity of He-Ne laser (I) was measured.

(11)The thickness of the thin film was controlled through the interference fringes. The thickness of this sample was 1265.6nm.

(12) The transmission spectrum of sample two was recorded in the region between (532-915 nm), by measuring ( $I_0$ ) and (I) before and after deposition of the layers above.

(13)The transmission, reflection, absorption coefficient and the refractive index, for this sample were calculated.

### **3-5-3 The procedure of sample three:**

Sample three consists of three layers .The first layer composed of Phenexazon, the second was Rhodamine 6G, while the third one was composed of Coumarin500.This sample was prepared as follows:

(1)The chamber was opened through the upper cover for replacing the substrate with another. The substrate put in  $45^\circ$  situation and the burettes were cleaned by applying the ethanol spirit.

(2)The chamber was closed carefully.

(3)The vacuum pump was turned ON, then the air was evacuated from the chamber till the pressure reach  $0.3 \times 10^{-2}$  mbar.

(4) Phenexazon was put in one of the burettes, and Rhodamin in the other. The valve of the first burette was open to deposited a layer from phenexazon, the laser signal was detected during the deposition, then the interference fringes were photographed, the deposition time was eleven seconds for deposition of one layer with thickness equal half the He-Ne wavelength.

(5)The valve of the first burette was turned OFF.

(6)The valve of the second burette that contains the solution of Rhodamine was open to deposit a layer from Rhodamine 6G on the same substrate and the same above steps were repeated, but the time here was twenty two seconds.

(7)Helium –neon laser was turned ON, and then the transmitted intensity (I) was measured by the digital multimeter, and the signal was detected by CRO.

(8) For obtaining a layer of Coumarin on the same substrate the Coumarin was put in the first burette, and deposition was done, within eleven seconds.

(9)Helium –neon laser was turned ON, and then the transmitted intensity (I) was measured by the digital multimeter, and the signal was detected by CRO.

(10)The transmitted intensity of He- Ne laser (I) was measured.

(11)The thickness of the thin film was controlled through the interference fringes. The thickness of this sample was 1265.6nm.

(12) The transmission spectrum of sample three was recorded in the region between (532-915 nm), by measuring ( $I_0$ ) and ( $I$ ) before and after deposition of the layers above.

(13) The transmission, reflection, absorption coefficient and the refractive index, for this sample were calculated.

#### **3-5-4 The procedure of sample four:**

Sample four consists of three layers. The first layer composed of Phenexazon, the second was Rhodamine 6G, while the third one was composed of Coumarin500. This sample was prepared as follows:

(1) The chamber was opened through the upper cover for replacing the substrate with another. The substrate put in 45 situation and the burettes were cleaned by applying the ethanol spirit.

(2) The chamber was closed carefully.

(3) The vacuum pump was turned ON, then the air was evacuated from the chamber till the pressure reach  $0.3 \times 10^{-2}$  mbar.

(4) Phenexazon was put in one of the burette, and Rhodamine in the other. The valve of the first burette was open to deposit a layer from phenexazon, the laser signal was detected during the deposition, then the interference fringes were photographed, the deposition time was measured, it was eleven seconds for deposition of one layer with thickness equal half the He-Ne wavelength. The deposition was done within twenty two seconds.

(5) The valve of the first burette was turned OFF.

(6)The valve of the second burette that contains the solution of Rhodamine 6G was open to deposit a layer from Rhodamine 6G on the same substrate and the same above steps were repeated.

(7)Helium –neon laser was turned ON, and then the transmitted laser intensity (I) was measured by the digital multimeter, and the signal was detected by CRO.

(8) For obtaining a layer of Coumarin on the same substrate the Coumarin was put in the first burette, and deposition was done, within eleven seconds.

(9)Helium –neon laser was turned ON, and then the transmitted intensity (I) was measured by the digital multimeter, and the signal was detected by CRO.

(10)The transmitted intensity of He-Ne laser (I) was measured.

(11)The thickness of the thin film was controlled through the interference fringes. The thickness of this sample was 1265.6 nm.

(12)The transmission spectrum of sample one was recorded in the region between (532-915 nm), by measuring ( $I_0$ ) and (I) before and after deposition of the layers above.

(13)The transmission, reflection, absorption coefficient and the, refractive index, for this sample were calculated.

### **3-5-5The procedure of sample five:**

Sample five consists of three layers .The first layer composed of Phenexazon, the second was Rhodamine 6G, while the third one was composed of Coumarin500. This sample was prepared as follows:

(1)The chamber was opened through the upper cover for replacing the substrate with another and the burette were cleaned by applying the ethanol spirit.

(2)The chamber was closed carefully.

(3)The vacuum pump was turned ON, then the air was evacuated from the chamber till the pressure reach  $0.3 \times 10^{-2}$  mbar.

(4)Phenexazon was put in one of the burettes, and Rhodamine in the other. The valve of the first burette was open to deposited a layer from phenexazon, the signal was detected during the deposition, then the interference fringes were photographed, the deposition time was computed, it was eleven second for deposition of one layer with thickness half the He-Ne wavelength. Then the thickness of one layer wasequal to 316.4 nm. The deposition time wastwenty two seconds.

(5)The valve of the first burette was turned OFF.

(6)The valve of the burette that contains the solution of Rhodamine 6G was open to deposit a layer from Rhodamine 6G on the same substrate and the same above steps were repeated.

(7)Helium –neon laser was turned ON, and then the transmitted laser intensity (I) was measured by the digital multimeter, and the signal was detected by CRO.

(8) For obtaining a layer of Coumarin on the same substrate the Coumarin was put in the first burette, and deposition was done, within twenty two second.

(9)Helium –neon laser was turned ON, and then the transmitted intensity (I) was measured by the digital multimeter, and the signal was detected by CRO.

(10)The thickness of the thin film was controlled through the interference fringes where each fringe means half- wavelength of the He-Ne laser (632.8nm). The thickness of this sample was  $(3 \lambda)$  which equal 1898.4 nm.

(11)The transmission spectrum of sample five was recorded in the region between (532-915 nm), by measuring  $(I_0)$  and (I) before and after deposition of the layers above.

(12)The transmission, reflection, absorption coefficient and the, refractive index, for this sample were calculated.

## CHAPTER FOUR

### Results and discussion

#### 4-1 Introduction:

This chapter presents and discusses the results obtained during the experimental work of this study. Some of the results were collected by measurement and the others were calculated.

This work was limited to the case of multilayers thin films deposited on substrates. After fabrication, the transmission spectra of these thin films were recorded in the range (532-915 nm).

Some wavelengths were transmitted and the others were reflected, according to the characteristics of the layers. The refractive index ( $n$ ) of the thin film and its absorption coefficient ( $\alpha$ ) was calculated using the equation below.

$$T+R +A =1 \quad (4-1)$$

Where (T) is the transmission, (R) is the reflectance;(A) is the absorbance of the thin film. The transmittance was calculated by the equation:

$$T = \frac{I}{I_0} \quad (4-2)$$

Where ( $I_0$ ) is incident laser intensity, and (I) is the transmitted laser intensity. The absorption coefficient can be obtained from Beer-Lambert law:

$$I = I_0 \exp \{-\alpha d\} \quad (4-3)$$

Where (d) is the thickness of the thin film, which was deduced experimentally using the interference fringes and ( $\alpha$ ) is the absorption coefficient. Also the refractive index (n) of each thin film was calculated from the equation:

$$n = \sqrt{n_s \times \left( \frac{1-\sqrt{R}}{1+\sqrt{R}} \right)}. \quad (4-4)$$

Where:

(n)is the refractive index of the thin film.( $n_s$ ) is the refractive index of the glass substrate which is equal to (1.3).

## 4-2 The samples results:

In this work, five samples were prepared from three dyes (Phenexazon, Rohdamin, Coumarin).

These samples were deposited on glass substrate with refractive index of 1.3.In the following table the components and thickness of the samples layers are presented:

**Table (4-1):The components and the thickness of the samples layers.**

Samples	The thickness (nm) of the components			The total thickness (nm)
	Phenexazon	Rohdamin6G	Coumarin	
S <sub>1</sub>	316.4	316.4	316.4	943.2
S <sub>2</sub>	316.4	316.4	632.8	1265.6
S <sub>3</sub>	316.4	632.8	316.4	1265.6
S <sub>4</sub>	632.8	316.4	316.4	1265.6
S <sub>5</sub>	632.8	632.8	632.8	1898.4

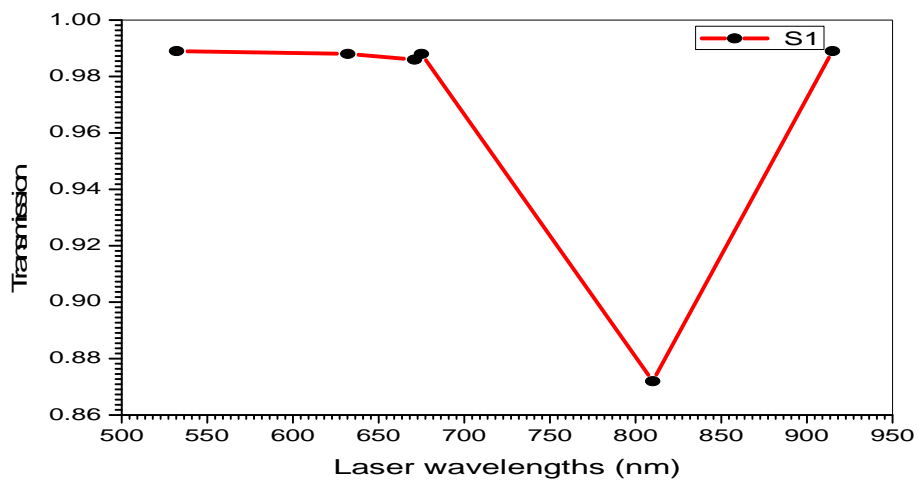
### 4-2-1Sample one (S<sub>1</sub>):

This sample was composed of three layers, the first layer was of Phenexazon, the second was of Rhodamine6G and the third was of Coumarin.

Table (4-2) lists the incident, transmitted intensities and reflectivity of different lasers for this sample. Figure (4-1) shows the transmission spectrum of sample  $S_1$  and table (4-3) lists the refractive index and the absorption coefficient of this sample.

**Table (4-2): The incident, transmitted intensity, the transmission and the reflectivity of sample  $S_1$**

$\lambda$ (nm)	$I_0$ (in volt)	$I$ (in volt)	T	R
532.0	1.012	1.001	0.989	0.0108
632.8	1.014	1.002	0.988	0.0118
671.0	1.016	1.004	0.986	0.013
675.0	1.015	1.003	0.988	0.012
820.0	1.019	1.006	0.872	0.0127
915.0	1.016	1.005	0.989	0.0108



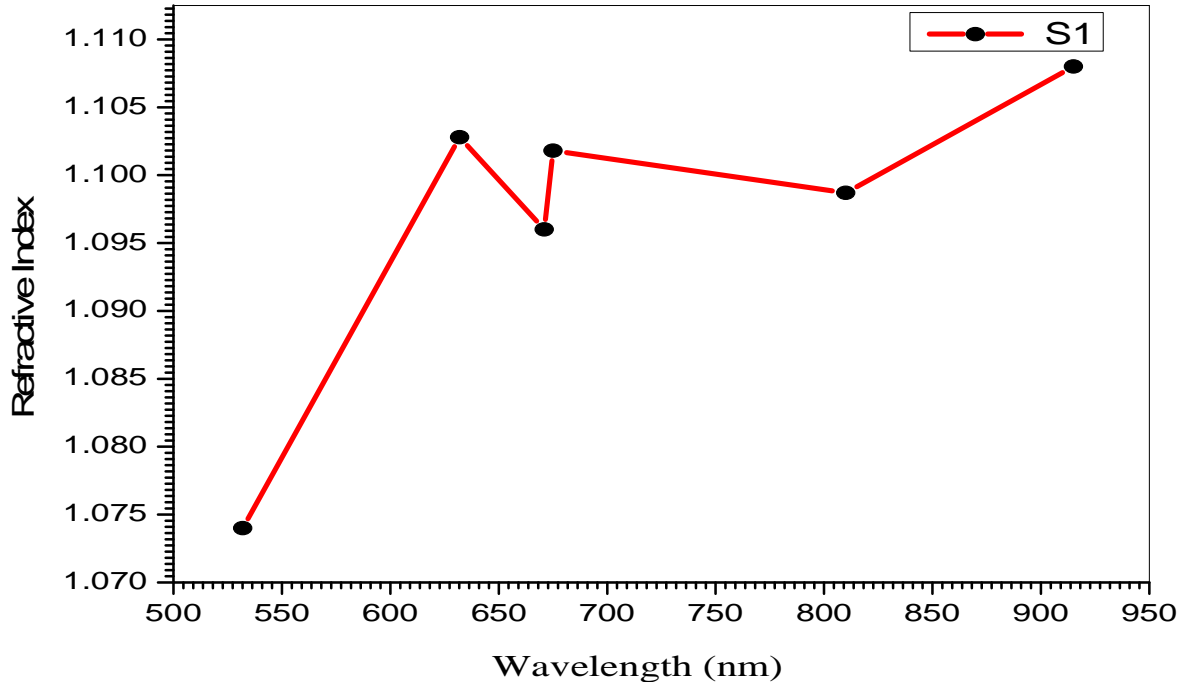
**Fig( 4-1): The transmission spectrum of sample  $S_1$**



It was found that the higher value of transmission is within the range (532-675 nm) also at the wavelength 915nm. Therefore this sample can be used as window. The lower value of transmission for this thin film was at wavelength of 820nm, so this sample can be used as reflector for this wavelength.

**Table(4-3): The refractive index and the absorption coefficient of sample S<sub>1</sub>**

$\lambda$ (nm)	n	$\alpha$ (cm <sup>-1</sup> )x10 <sup>-4</sup>
532.0	1.074	1.151
632.8	1.1028	1.246
671.0	1.096	1.251
675.0	1.1018	1.252
820.0	1.0987	1.35
915.0	1.108	1.142



**Fig(4-2): The refractive index of sample S<sub>1</sub> versus wavelength**

Figures (4-2) and (4-3) show the relationship between the refractive index, the absorption coefficient of  $S_1$  and wavelengths. The highest value of refractive index was found at 915 nm, and the lowest was at 532 nm. Sample one can be used within the range between 632 up to 915 nm as a reflector.

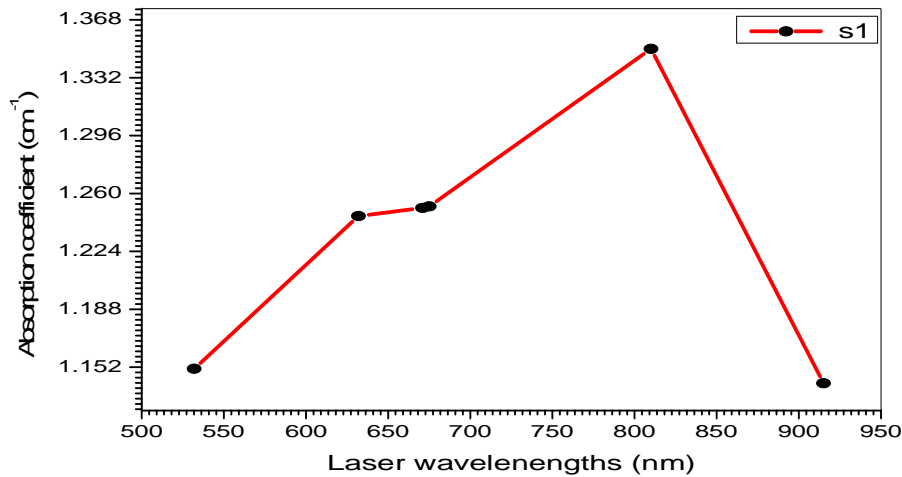


**Figure (4-3): The absorption coefficient at different wavelengths for sample one.**

From fig: (4-3) one can noticed that sample  $S_1$  have higher value for absorption coefficient at 820 nm, so it can be used as an absorption filter in this wavelength. The lower value of its absorption coefficient was at (915, 532.8 nm). At these wavelengths sample  $S_1$  can be used as transmitted filter.

#### 4-2-2 Sample two ( $S_2$ ):

It contains three layers, one of the Phenexazon dye, the second of Rhodamin, and the third layer of the Coumarin dye. Table (4-4) lists the incident, the transmitted intensities, the reflectivity and transmission of this thin film for different lasers wavelenghtes, while table (4-5) lists the refractive index and the absorption coefficient for the same sample. Figure (4-4) shows the transmission spectrum of sample two.

**Table(4-4): The incident, transmitted intensity, the transmission and the reflectivity of sample S<sub>2</sub>**

$\lambda$ (nm)	$I_o$ (in volt)	$I$ (in volt)	T	R
532.0	1.001	0.97	0.969	0.0309
632.8	1.002	0.973	0.97105	0.0289
671.0	1.004	0.98	0.976	0.0239
675.0	1.003	0.983	0.98	0.0199
820.0	1.0054	0.988	0.9826	0.0173
915.0	1.0023	0.975	0.9727	0.027

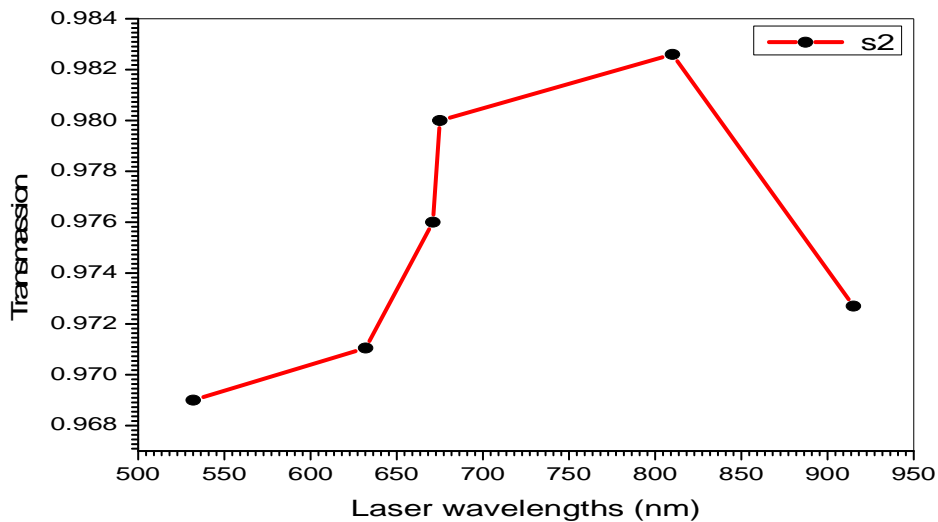
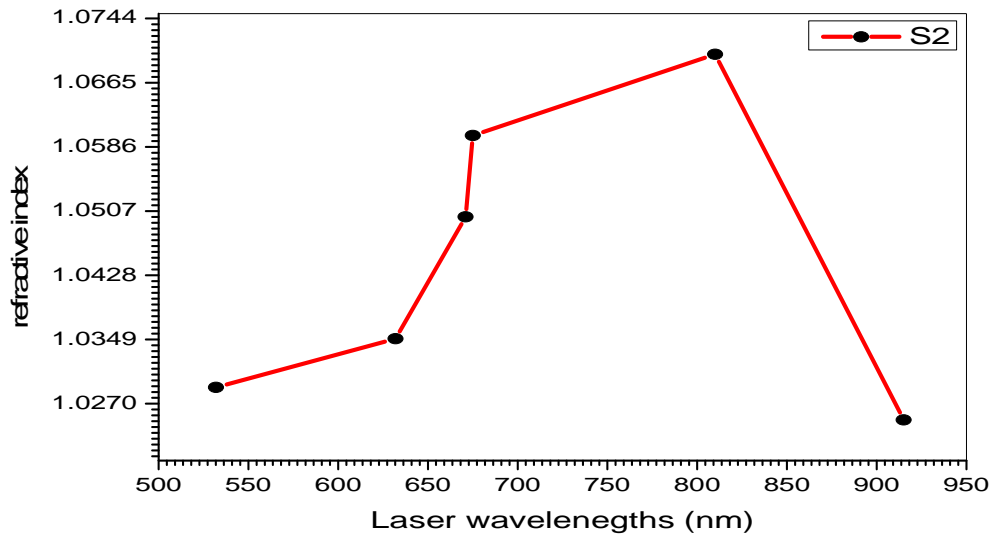


**Fig (4-4): The transmission spectrum of sample two.**

It can be noticed from figure (4-4) that the transmission for this sample is maximum at wavelength of 820nm, which means that this sample can be used as a window for this wavelength. From the same figure one can see that this sample can be used as reflector or partial reflector in the region from 532nm to 632nm where the transmission was lower compared with other wavelengths.

**Table(4-5): The refractive index and the absorption coefficient of sample S<sub>2</sub>**

$\lambda$ (nm)	n	$\alpha(\text{cm}^{-1}) \times 10^{-4}$
532.0	1.029	2.41
632.8	1.035	2.08
671.0	1.05	1.873
675.0	1.06	1.588
820.0	1.07	1.37
915.0	1.025	2.18



**Fig( 4-5): The refractive index of sample S<sub>2</sub> versus wavelength**

Figure (4-5) shows the refractive index of sample two as a function of wavelengths. It was found that the highest value of the refractive index was at 820nm, and the lowest value was 915nm. Sample two can be used for a reflector within the range 671 up to 820nm. But at the range 532 to 632nm and the wavelength 915nm, sample two can be used as a partial reflector.

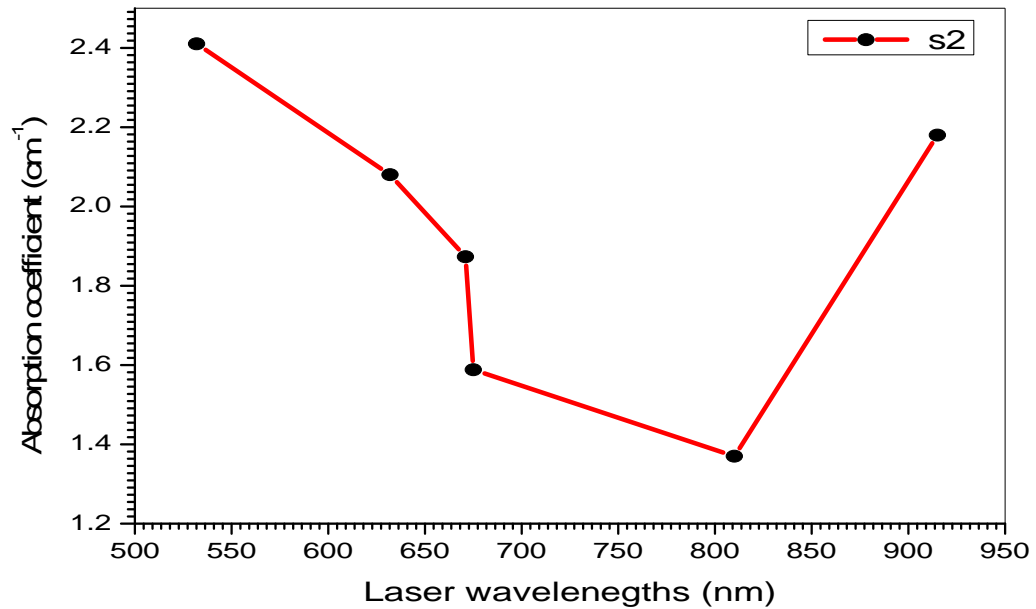


**Fig (4-6):The absorption coefficient of sample S<sub>2</sub> versus lasers wavelengths**

From figure (4-6) it can be observed that the least value for absorption coefficient is at (820 nm) compared to the other wavelengths. Indeed the sample at this wavelength can be used as reflector. Also the values of the absorption coefficient increased at other wavelengths compared to (820nm), and reach the highest value at (532.8 nm). This feature means that this sample can be used as an absorption filter at (532 nm).

#### **4-2-3 Sample three (S<sub>3</sub>):**

This sample also contains three layers as follows: One layer of the first

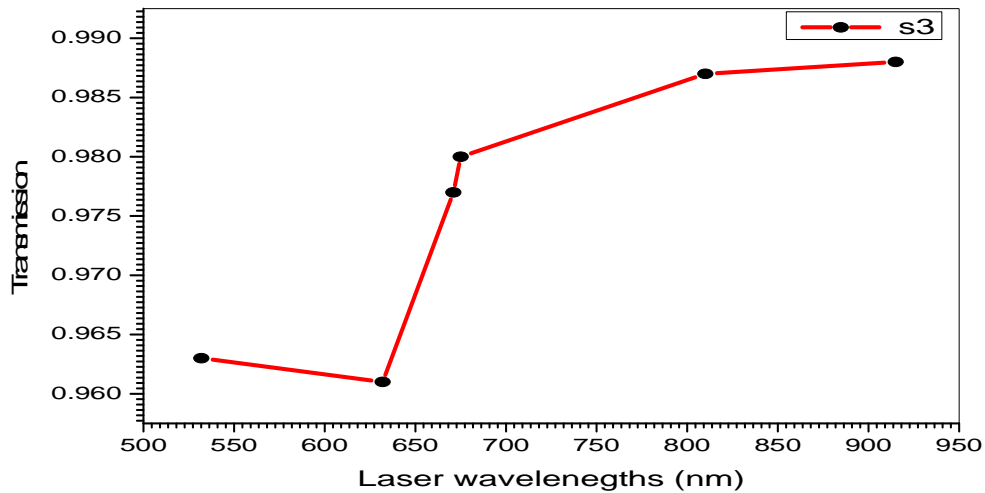
Dye(phenexazon), the second layer of Rhodamin and last one of the Coumarin.

Table (4-6) lists the incident, transmitted intensities, reflectivity and transmission of the thin film for different laser wavelengths, while table (4-7) lists the refractive index and the absorption coefficient of this sample.

Figure (4-7) shows the transmission spectrum of sample S<sub>3</sub>.

**Table (4-6): The incident, transmitted intensity, the transmission and reflectivity of sample S<sub>3</sub>**

$\lambda$ (nm)	$I_0$ (in volt)	I(in volt)	T	R
532.0	1.05	1.012	0.963	0.036
632.8	1.015	0.976	0.961	0.038
671.0	1.002	0.979	0.977	0.022
675.0	1.001	0.981	0.98	0.02
820.0	1.002	0.989	0.987	0.013
915.0	1.003	0.991	0.988	0.011



**Fig( 4-7):The transmission spectrum of sample S<sub>3</sub>**

The highest value of transmission is at the 915nm and the lowest value is in the range between 532-632nm. This sample can be used as a window at the range between 671 up to 915nm, but at 532 to 632nm this sample can be used as reflector.

**Table (4-7): Therefractive index and theabsorption coefficient of sampleS<sub>3</sub>**

$\lambda$ (nm)	n	$\alpha(\text{cm}^{-1}) \times 10^{-4}$
532.0	1.015	2.908
632.8	1.0105	3.091
671.0	1.05	1.79
675.0	1.066	1.58
810.0	1.08	1.031
915.0	1.107	1.39

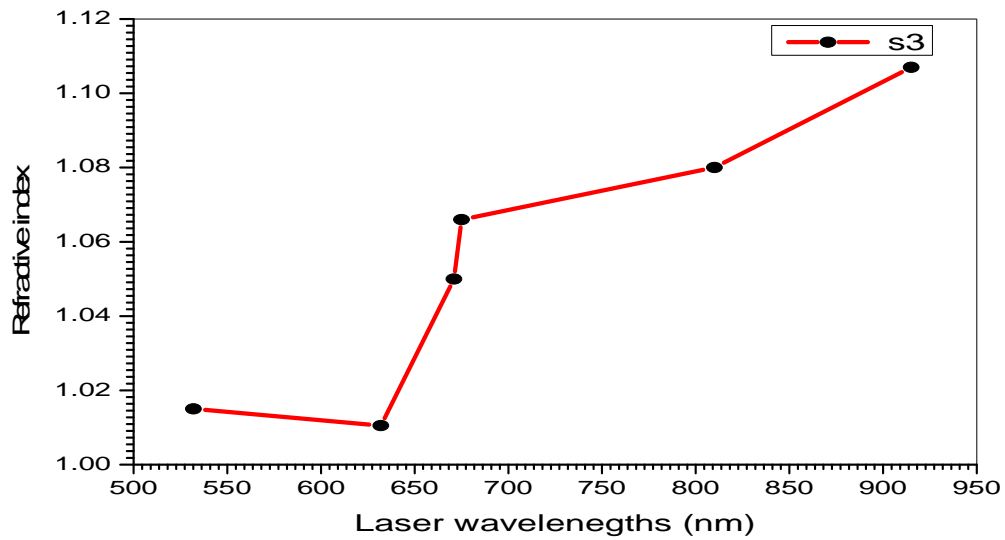


**Figure (4-8):Therefractive index of sample S<sub>3</sub> versus laser wavelength**

One can be noticed that the maximum value of refractive index at the wavelength the region 671 to 915nm,it means that this sample can be used as,a reflector. The minimum value of refractive index at the wavelengths 532 up to 632 nm also this sample can be used as a partial reflector.

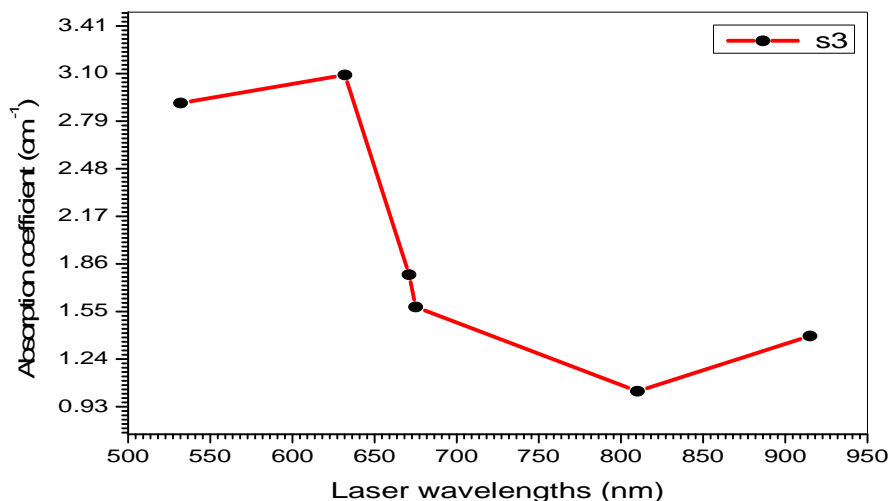


**Fig (4-9): The absorption coefficient of sample S<sub>3</sub> versus laser wavelengths.**

Figure 4-9 shows that the absorption coefficient was changed with the changing of wavelength. At the wavelength of 632 nm we obtained the maximum value of absorption coefficient, so that this sample can be used as absorption filter. The minimum value of the absorption coefficient was obtained at 820 nm and it can be used as reflector filter.

#### **4-2-4 Sample four (S4):**

It contains three layers, the first of Phenexazon dye and the second was of Rhodamin and the last one of Coumarin.

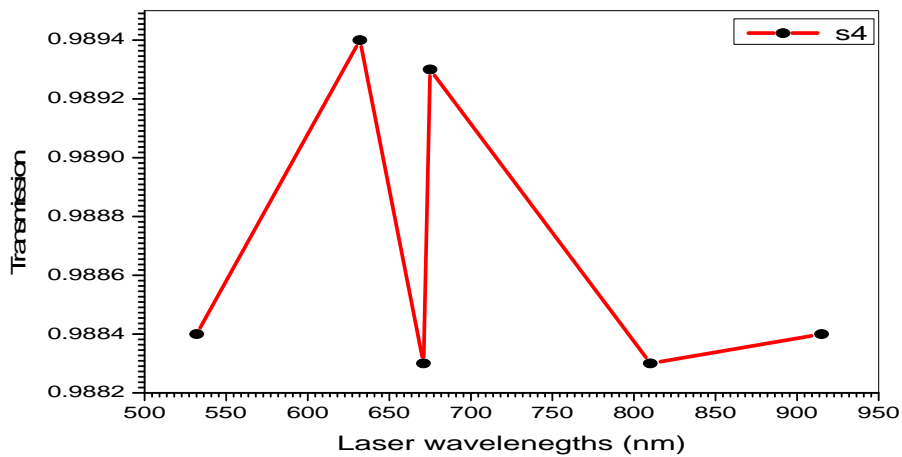
Table (4-8) lists the incident, transmitted intensities, reflectivity and transmission of this thin film of different laser wavelengths, while table (4-9) lists the refractive index and the absorption coefficient for the same sample.

Figure (4-10) shows the transmission spectrum of sample four.



**Table (4-8): The incident, transmitted intensity, the transmission and reflectivity of sample S<sub>4</sub>**

$\lambda$ (nm)	I <sub>0</sub> (in volt)	I (in volt)	T	R
532.0	1.107	1.023	0.9884	0.011
632.8	1.112	1.028	0.9894	0.01
671.0	1.103	1.021	0.9883	0.0116
675.0	1.109	1.022	0.9893	0.0106
820.0	1.094	1.018	0.9883	0.0135
915.0	1.038	1.026	0.9884	0.0115



**Fig( 4-10): The transmission spectrum of sample S<sub>4</sub>**

It can be noticed that the transmission for this sample is maximum at the wavelengths 632,675nm, which means that this sample can be used as a window for these wavelengths. But the minimum value of the transmission at(532,671) nm and at the range between (820 to915 nm),then this sample at these wavelengths can be used as reflector.

**Table (4-9):The refractive index and the absorption coefficient of sample S<sub>4</sub>**

$\lambda$ (nm)	n	$\alpha(\text{cm}^{-1}) \times 10^{-4}$
532.0	1.107	9.19
632.8	1.112	8.409
671.0	1.103	7.079
675.0	1.109	8.409
820.0	1.094	9.19
915.0	1.1039	9.183

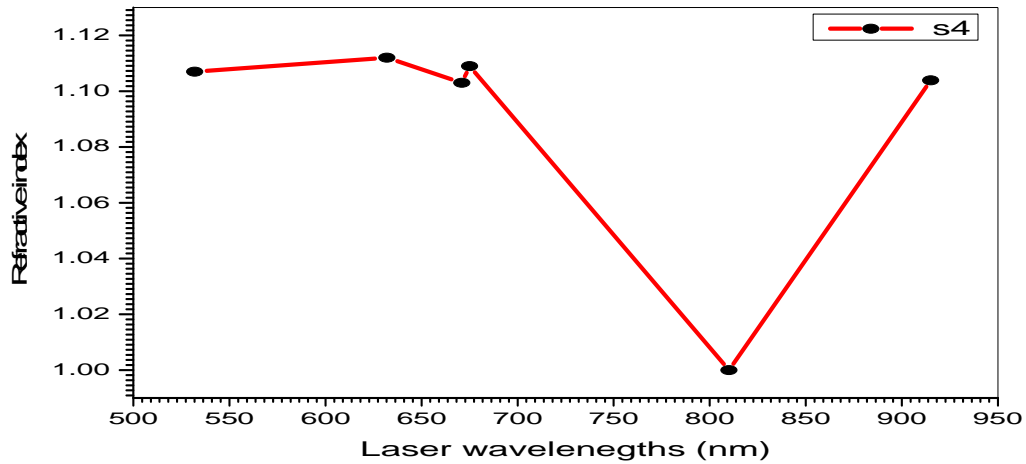


**Fig (4-11):The refractive index of sample S<sub>4</sub> versus laserwavelength**

Figure (4-11) illustrates the refractive index for sample four. The region of the high value of refractive index was equal 532 up to 675nm, and also at the wavelength 915nm, it means that this sample can be used as a reflector at these wavelengths. But the low value of refractive index at 820nm compared to other wavelengths, it means that this sample can be used as a partial reflector.

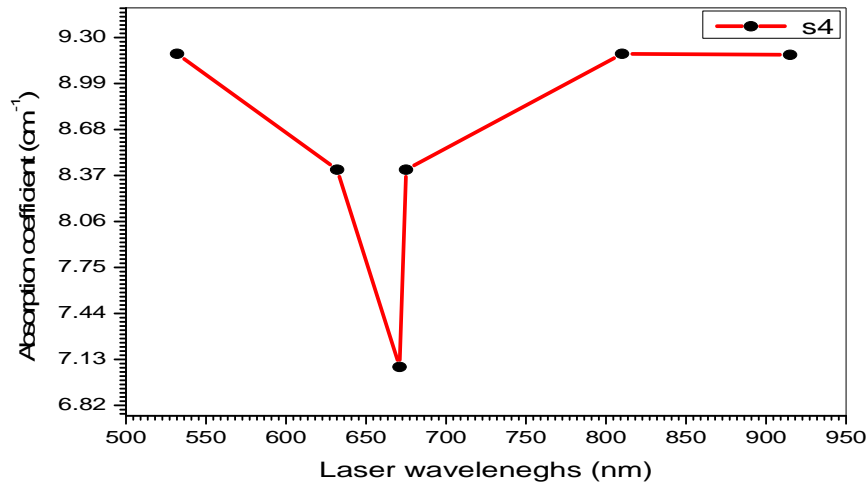


**Fig (4-12): The absorption coefficient of sample S<sub>4</sub> versus laserwavelength.**

In fig (4-12) one can observed that the lower value of the absorption coefficient is at (671 nm), then this sample at this wavelength can be used as transmitted filter.

At the other wavelengths, the absorption coefficient is increased until its higher value at (532 nm), and (820, 915 nm).

From this result this sample can be used as an absorption filter in these wavelengths.

#### **4-2-5 Sample five (S<sub>5</sub>):**

It contains three layers, the first layer was of Phonoexazon, the second was of Rohdamin6G and the third was of Courmarin. Table (4-10) lists the incident, transmitted intensities, reflectivity and transmission of the thin film for different laser wavelengths. Table (4-11) lists refractive index and the absorption coefficient of sample five. Figure (4-13) shows the transmission spectrum of the same sample.

**Table (4-10): The incident, transmitted intensity, the transmission and reflectivity of sample S<sub>5</sub>**

$\lambda$ (nm)	$I_0$ (in volt)	I (in volt)	T	R
532.0	1.002	0.986	0.984	0.015
632.8	1.001	0.987	0.986	0.0139
671.0	1.0014	0.988	0.9866	0.0133
675.0	1.0015	0.987	0.985	0.014
810.0	1.0022	0.989	0.9868	0.01317
915.0	1.003	0.986	0.983	0.0169

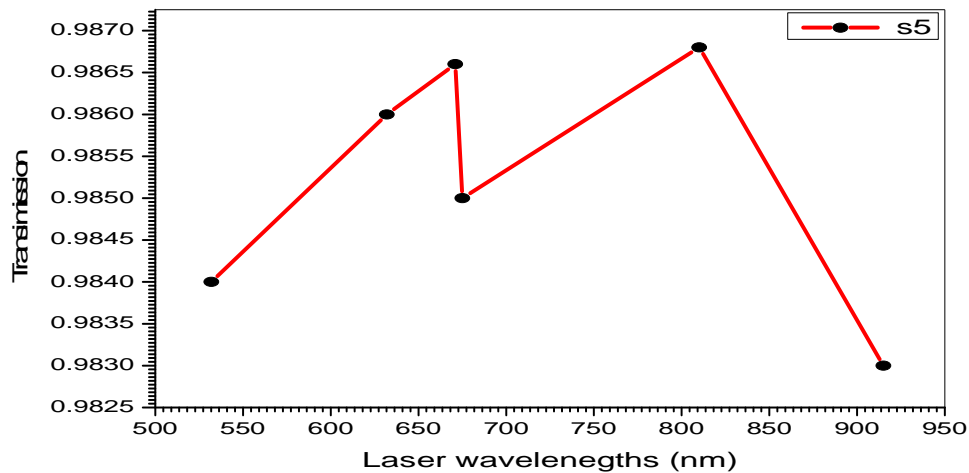


**Fig (4-13):The transmission spectrum of sample S<sub>5</sub>.**

The highest value of the transmission, within the range 532 to 820nm, means that this sample can be used as a window. But the lowest value at wavelength of 915nm, compared with other wavelengths, means that it can be used as reflector at this wavelength.

**Table (4-11): The refractive index and the absorption coefficient of sample S<sub>5</sub>**

$\lambda$ (nm)	n	$\alpha$ (cm <sup>-1</sup> ) x10 <sup>-4</sup>
532.0	1.08	8.36
632.8	1.093	7.375
671.0	1.095	7.096
675.0	1.09	7.635
820.0	1.096	6.959
915.0	1.079	8.983

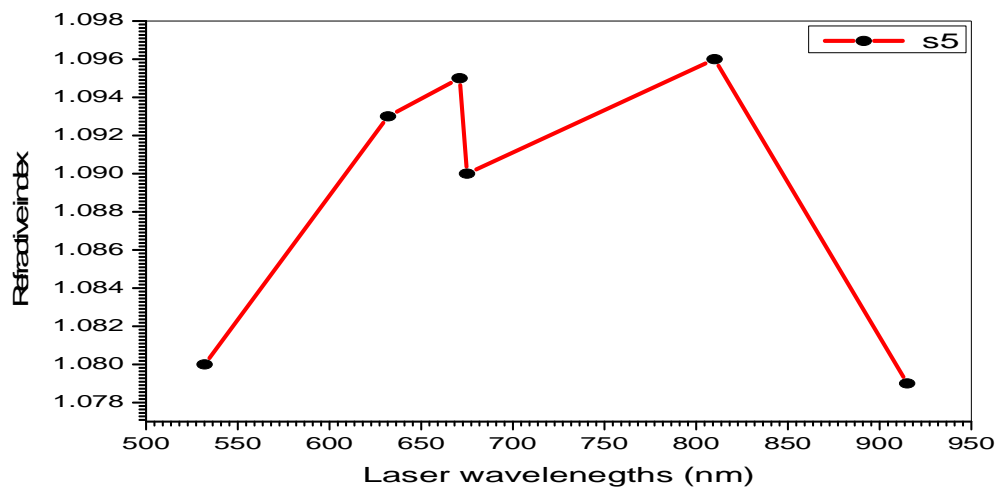


**Fig (4-14): The refractive index for sample S<sub>5</sub> versus laser wavelength**

Figure(4-14) shows the refractive index for sample five. The highest value of refractive index is at 632 to 820nm, so it can be used as a partial reflector. But the lowest value of refractive index at 532,915nm means that this sample can be used as a reflector at this wavelength.

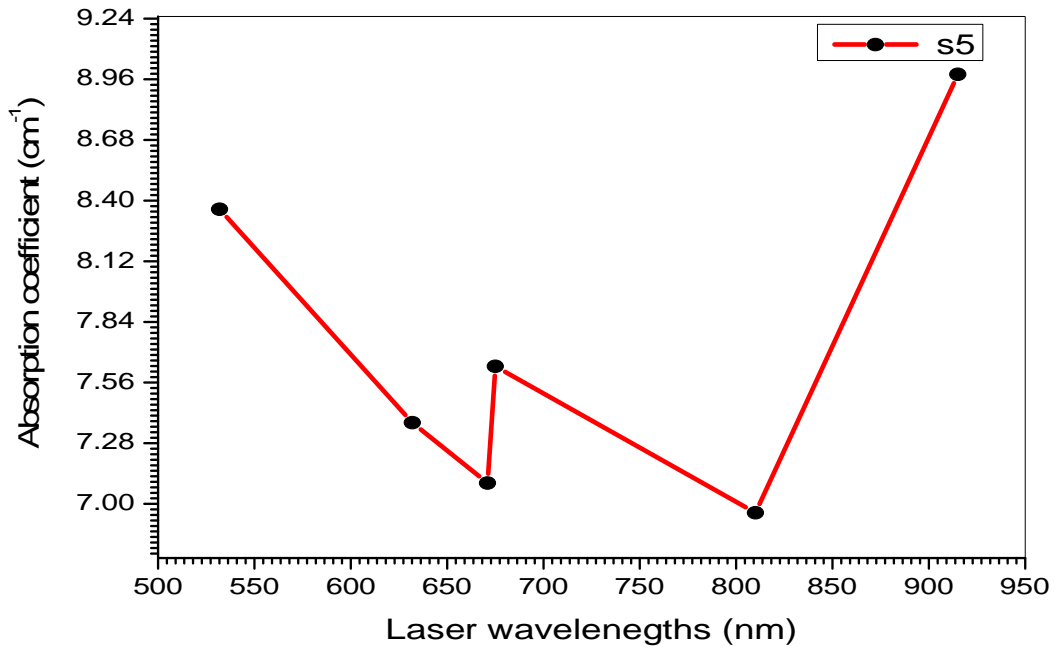


**Fig (4-15): The absorption coefficient of sample S<sub>5</sub> versus lasers wavelengths.**

Figure (4-15) shows the absorption coefficient of sample five at different wavelengths, it can be noticed that the higher value is at (915 nm) then this sample can be used as an absorption filter in this wavelength. The lower is at (820 nm) to (671 nm) so it can be used as transmitted filter.

#### **4-3.Comparison between the optical propertiesof the fivesamples:**

The optical properties of the five samples are presented in the following tables in the wavelength range 532 to 915 nm.

##### **4-3-1: The transmission of the five samples:**

Table(4-12) illustrates a comparison between the transmission of the fivesamples in the range532to 915 nm.

**Table (4-12): The transmission of the five samples.**

$\lambda$ ( nm)	T (S <sub>1</sub> )	T (S <sub>2</sub> )	T (S <sub>3</sub> )	T (S <sub>4</sub> )	T (S <sub>5</sub> )
532.0	0.989	0.969	0.963	0.988	0.984
632.8	0.988	0.971	0.961	0.989	0.986
671.0	0.956	0.976	0.977	0.988	0.986
675.0	0.988	0.980	0.980	0.989	0.985
820.0	0.967	0.982	0.987	0.983	0.9868
915.0	0.989	0.972	0.988	0.9884	0.983

**4-3-2.The reflectivity of the five samples:**

Table (4-13) indicates a comparison between the reflectivity of the five samples in the range between 532 nm and 915 nm

**Table(4-13): The reflectivity of the five samples**

$\lambda$ ( nm)	R (S <sub>1</sub> )	R(S <sub>2</sub> )	R(S <sub>3</sub> )	R(S <sub>4</sub> )	R(S <sub>5</sub> )
532.8	0.0198	0.0309	0.036	0.011	0.015
632.8	0.0118	0.0289	0.0380	0.010	0.0139
671.0	0.0130	0.0239	0.022	0.0116	0.0133
675.0	0.0120	0.0199	0.020	0.0106	0.014
820.0	0.0127	0.0173	0.0130	0.0135	0.0132
915.0	0.0108	0.0270	0.011	0.0115	0.0169

**4-3-3The Refractive indicesof the five samples:**

The refractive indicesof the five samples in the same previous spectral range are presentedintable (4-14).

**Table (4.14): The refractive index of the five samples**

$\lambda$ ( nm)	n (S <sub>1</sub> )	n (S <sub>2</sub> )	n (S <sub>3</sub> )	n (S <sub>4</sub> )	n (S <sub>5</sub> )
532.0	1.074	1.029	1.015	1.107	1.80
632.8	1.1028	1.035	1.0105	1.112	1.093
671.0	1.096	1.050	1.050	1.103	1.095
675.0	1.1018	1.060	1.066	1.109	1.090
820.0	1.098	1.070	1.080	1.094	1.096
915.0	1.108	1.10	1.107	1.103	1.079

**4-3-4: The absorption coefficients of the five samples**

Table (4-15) list the absorption coefficients of the five samples in the range between 532 and 915 nm.

**Table (4-15): The absorption coefficients of five samples.**

$\lambda$ ( nm)	$\alpha(S_1) \times 10^{-4} \text{ cm}^{-1}$	$\alpha(S_2) \times 10^{-4} \text{ cm}^{-1}$	$\alpha(S_3) \times 10^{-4} \text{ cm}^{-1}$	$\alpha(S_4) \times 10^{-4} \text{ cm}^{-1}$	$\alpha(S_5) \times 10^{-4} \text{ cm}^{-1}$
532.0	1.151	2.410	2.908	9.190	8.360
632.8	1.246	2.080	3.091	8.409	7.375
671.0	1.251	1.873	1.790	7.079	7.096
675.0	1.252	1.588	1.580	8.409	7.635
820.0	1.350	1.370	1.031	9.190	6.959
915.0	1.142	1.180	1.390	9.183	8.983

**4.4 The Discussion:**

The comparison between figure (4-4) and figure (4-7) show that there is a slight increase in the transmission of sample three than sample two in the region between (820 and 915) nm. So sample three can be used to get good filter in this region.



Figure(4-7) and (4-10) show that there is an increase in the transmission of sample three than sample four in the region (675 to 915) nm and also between (632.8 to 675) nm. Since the three samples (two, three and four) have equal thickness, then the difference of the values of transmission come from the difference of materials in each sample. It can be noticed in figures (4-5) and

(4-8) that the refractive index ( $n$ ) of sample three is higher than the refractive index of sample two at the region (820 to 915) nm.

Figures (4-5) and (2-11) showed the variation of the refractive index ( $n$ ) with laser wavelengths for sample two and four. These figures showed that the refractive index of sample four is higher than the refractive index of sample two at the region (532 to 632.8) nm. The difference between the refractive index of sample two and three, and sample two and four comes from the difference of the sort of the layers of each sample.

Figures (4-6) and (4-9) show the absorption coefficient as a function of wavelength for samples two and three, respectively. They are similar in the region between (632.8 to 820) nm, but there is a slight increase of absorption coefficient of sample two at the region (820 – 915) nm. Also figures (4-6) and (4-12) show the absorption coefficient of sample two and sample four, respectively. They are similar in the region from (532 to 632.8) nm and from (820 to 915) nm, but there is a slight increase of absorption coefficient of sample four and that is because of the different layers in each sample.

Figures (4-1) and (4-13) show the transmission spectra of sample one and sample five, respectively, there is a difference at the region (675 to 820) nm and (820 to 915) nm. The transmission increase in sample one than sample five at that wavelengths. The variations are depending on the difference of the thickness of these samples.

Figures (4-2) and (4-14) show the refractive index ( $n$ ) of sample one and sample five. They are similar in the region (532 to 632.8) nm, but there is a slight increase of refractive index for sample one than sample five at the region (820 to 915) nm. These differences are due to the difference of materials in the two samples.

Figures (4-3) and (4-15) show the absorption coefficient of sample one and sample five, respectively. There is a slight increase in the absorption coefficient of sample five than sample one at the region (820 to 915) nm.

Table (4-12) shows a comparison between the five samples at the wavelengths (532 to 915) nm. These data give a good indication to use these samples as absorption filters.

Table (4-13) lists the reflectivity of five samples at different wavelengths. The reflectivity of sample one and five are similar in the region (632 to 915) nm, but the reflectivity of samples (two, three and five) are different because of the differences in the thickness of the layers. Sample one and sample five can be used as reflectors and other samples can be used as partial reflectors.

Table (4-14) lists the refractive indices of the five samples at various wavelengths. The comparison shows that the refractive indices are similar in the region (532 to 915) nm for sample one and sample five and different for sample two, sample three and sample five, then sample one and sample five can be used as filters.

Table (4-15) lists the absorption coefficients of the five samples. The comparison shows that the absorption coefficient is low for sample one and sample two, they can be used as filters (Suliman.E.M., 2007). But sample four and sample five can be used as reflectors because their absorption coefficients are high in region (532 to 915) nm.

## 4-5 Conclusions:

From the obtained results, one can conclude that:

1. Multilayers thin films were fabricated successfully from liquids deposited on substrate.
2. There is a slight increase in the transmission of sample three than sample two in the region between (820 and 915) nm.
3. There is an increase in the transmission of sample three than sample four in the region (675 to 915) nm and also between (633 to 675) nm.
4. The transmission in the region (675 to 820) nm and (820 to 915) nm is higher for sample one compared with sample five.
5. The reflectivities of sample one and five are similar in the region (632.8 to 915) nm, but the reflectivities of samples (two, three and five) are different.
6. The absorption coefficients of samples one, two and three are low compared with sample four and sample five.
7. When the absorption coefficient increased the refractive index decreased.
8. The difference in the transmission, reflectivity, refractive indices and absorption coefficients of the films is referred to the sort or the thickness of layers.
9. The thickness of the deposited liquid samples can be controlled and measured via interference fringes of the transmitted laser light.
10. The three materials can be used to produce optical components in the region (532 to 915) nm.

## **4-6 Recommendations:**

For obtaining better results it is recommended to apply the followings:

- 1- Fabrication of multilayers thin films composed of other materials like:  
Oxides, Fluorides.
- 2- Fabrication of multilayers thin films with large number of layers each with a thickness of  $532/2$  nm.

## 4.7References:

Aasi, J., Abbott, Abernathy, M.R., Ackley, K., Adams, C., Adams, T., Addesso, P., Adhikari, R.X. and Adya, V., (2015). Advanced ligo. *Classical and Quantum Gravity*, 32(7), p.074001.

Aad, G., Abdallah, J., Khalek, S.A., Abidinov, O., Abi, B., Abolins, M., AbouZeid, O.S., Abramowicz, H., (2014). Search for squarks and gluinos with the ATLAS detector in final states with jets and missing transverse momentum using proton-proton collision data. *Journal of high energy physics*, pp.1-52.

Aad, G., Abdallah, J., Abdelalim, A.A., Abdesselam, A., Abidinov, O., Abi, B., Abolins, M., Abramowicz, H., Abreu, H. and Acerbi, E.,( 2012). Measurement of the cross section for the production in association with b-jets in pp collisions at with the ATLAS detector. *Physics Letters B*, 707(5), pp.418-437.

Bárcena, C., Sra, A.K. and Gao, J., (2009). Applications of magnetic nanoparticles in biomedicine. In *Nanoscale magnetic materials and applications* (pp. 591-626). Springer US.

Bates, J.B., Dudney, N.J., Neudecker, B., Ueda, A. and Evans, C.D.,( 2000). Thin-film lithium and lithium-ion batteries. *Solid State Ionics*, 135(1), pp.33-45.

Brownlee, MD, M., (1995). Advanced protein glycosylation in diabetes and aging. *Annual review of medicine*, 46(1), pp.223-234.

Bednarek, J.R.D. and Launius, R.D. eds.,( 2003). *Reconsidering a century of flight*. UNC Press Books.

Buttry, D.A. and Ward, M.D.,( 1992).Measurement of interfacial processes at electrode surfaces with the electrochemical quartz crystal microbalance.*Chemical Reviews*, 92(6), pp.1355-1379.

Christopher, M.B. and Ana, M.O.B., (1993). Electrochemistry: principles, methods, and applications. *Oxford University Press*, 12, p.260.

Chopra, K.N. and Maini, A.K.,( 2010). *Thin films and their applications in military and civil sectors*. Defence Research and Development Organisation, Ministry of Defence.New Delhi.

Chopra, K.N., (2013). A short note on the organic semiconductors and their technical applications in Spintronics. *Lat. Am. J. Phys. Educ. Vol*, 7(4), p.674.

- Davis, W.J., Lehmann, P.Z. and Li, W., (2015). Nuclear PI3K signaling in cell growth and tumorigenesis. *Frontiers in cell and developmental biology*, 3, p.24.
- Dobrowolski, J.A.,( 1995). Optical properties of films and coatings. Handbook of optics, 1, pp.42-3.
- Evans, A.G. and Hutchinson, J.W.,( 1984). On the mechanics of delamination and spalling in compressed films. *International Journal of Solids and Structures*, 20(5), pp.455-466.
- Felton, L.A. and Porter, S.C.,( 2013). An update on pharmaceutical film coating for drug delivery. *Expert opinion on drug delivery*, 10(4), pp.421-435.
- Grove, E.L. And Perkins, A.J.,( 2012). *Developments in Applied Spectroscopy* (Vol. 9). Springer Science &Business Media.
- Jones, M.G., Gardner, G.E., Falvo, M. and Taylor, A., (2015). Precollege nanotechnology education: a different kind of thinking. *Nanotechnology Reviews*, 4(1), pp.117-127.
- Krishna, S., (2002). Handbook of Thin-film Deposition Processes and Techniques.2<sup>nd</sup> edition. Santa Clara, California.
- Kowalczewski, P., Bozzola, A., Liscidini, M. and Andreani, L., (2014). Light trapping and electrical transport in thin-film solar cells with randomly rough textures. *Journal of Applied Physics*, 115(19), p.194504.
- Kuo, Y., (2013). Thin Film Transistor Technology--Past Present and Future.*Electrochemical Society Interface*, 22(1), pp.55-61.
- KUMAR, G.S. and RAO, J.V.R., COMPARISON OF JE CHARACTERISTICS OF A CNT BASED COLD CATHODE GROWN BY CVD AND PECVD. *International Journal of Metallurgical & Materials Science and Engineering*, 1(3), pp.17-22.
- Li, J. and Zhang, J.Z.,( 2009). Optical properties and applications of hybrid semiconductor nanomaterials. *Coordination Chemistry Reviews*, 253(23), pp.3015-3041.
- Meakin, P., (1998). *Fractals, scaling and growth far from equilibrium* (Vol. 5). Cambridge university press.

Magnfält, D., (2014). Fundamental processes in thin film growth: The origin of compressive stress and the dynamics of the early growth stages.

Martin, J.I., Nogues, J., Liu, K., Vicent, J.L. and Schuller, I.K.,( 2003). Ordered magnetic nanostructures: fabrication and properties. *Journal of magnetism and magnetic materials*, 256(1), pp.449-501.

Palasantzas, G. and Backx, G.M.E.A.,( 2003). Wetting of van der Waals solid films on self-affine rough surfaces. *Physical Review B*, 68(3), p.035412.

Ramachandran, V.S., Paroli, R.M., Beaudoin, J.J. and Delgado, A.H., (2002).*Handbook of thermal analysis of construction materials*. William Andrew.

Richter, C., Wu, Z., Panaitescu, E., Willey, R.J. and Menon, L.,( 2007). Ultra-High-Aspect-Ratio Titania Nanotubes. *Advanced Materials*, 19(7), pp.946-948.

Stenzel, O.,( 2005). *The Physics of thin film optical spectra* (p. 116ff). Springer.New York.

Suliman. E.E.,( 2007). Utilization of Different Laser Systems to Determine the Optical Properties of Chloroform and Rhodamine 6G Thin–Films in Nanometer Scale (Master dissertation, sudan university of science and technology).Sudan.

Shaw, G.A., Trethewey, J.S., Johnson, A.D., Drugan, W.J. and Crone, W.C., (2005). Thermomechanical High-Density Data Storage in a Metallic Material Via the Shape-Memory Effect. *Advanced Materials*, 17(9), pp.1123-1127.

Sarakinos, K., Magnfält, D., Elofsson, V. and Lü, B., (2014). Atomistic view on thin film nucleation and growth by using highly ionized and pulsed vapour fluxes. *Surface and Coatings Technology*, 257, pp.326-332.

Thomas, N.L., (1991). The barrier properties of paint coatings. *Progress in Organic Coatings*, 19(2), pp.101-121.

Teichert, C., (2002). Self-organization of nanostructures in semiconductor heteroepitaxy. *Physics Reports*, 365(5), pp.335-432..

Venturi, D., Cho, H. and Karniadakis, G.E., (2015). Mori-Zwanzig Approach to Uncertainty Quantification.

WANG, L.D., Min, L., ZHANG, T.H. and LIANG, N.G., (2003). Hardness measurement and evaluation of thin film on material surface. Chinese Journal of Aeronautics, 16(1), pp.52-58.